APPLICATION OF THE TRANSPIRATION METHOD FOR EFFICIENT AEROELASTIC ANALYSIS USING AN EULER SOLVER

By

CLINT COLEMAN FISHER

Bachelor of Science

Oklahoma State University

Stillwater, Oklahoma

1993

Submitted to the Faculty of the
Graduate College of the
Oklahoma State University
in partial fulfillment of
the requirements for
the Degree of
MASTER OF SCIENCE
May, 1996

APPLICATION OF THE TRANSPIRATION METHOD

FOR EFFICIENT AEROELASTIC ANALYSIS

USING AN EULER SOLVER

Thesis Approved:

Thesis Advisor

Dean of the Graduate College

ACKNOWLEDGMENTS

I would foremost like to express my deep gratitude to my major advisor, Dr. Andrew Arena for his guidance and for the tremendous opportunity that he gave me. His assistance and direction were invaluable. I would also like to thank my committee members, Dr. David Lilley and Dr. Peter Moretti.

Funds for the support of this study have been allocated through the NASA-Ames University Consortium Office, under Interchange Number NCC2-5105, and Oklahoma State University. I wish to express my sincere appreciation to these funding organizations and to the technical director of the study, Dr. Kajal K. Gupta of the Dryden Flight Research Center.

I would also like to give my appreciation to the Department of Mechanical and Aerospace Engineering for granting me teaching assistantships that helped support me during my graduate studies.

Finally, I would like to thank my parents for their support, motivation, and continuous encouragement.

TABLE OF CONTENTS

Section Page

1. INTRODUCTION 1

1.1. Background 1
1.2. Problem Statement 2
1.3. Motivation for the Study 3
1.4. Rationale 6
1.5. Flutter Analysis 6
1.6. Literature Review 7
1.6.1. Transpiration Concept 7
1.6.2. Transpiration in Full Potential Studies 8
1.6.3. Transpiration in Euler Studies 11
1.7. Objectives of the Present Study 14

2. METHODOLOGY 16

2.1. Transpiration Development 16
2.2. Steady Panel Methods 18
2.3. STARS Code 19
2.3.1. Flow Solver 21
2.3.2. Aeroelastic and Aeroservoelastic Solver 22
2.3.3. Code Modifications 24
2.3.3.1. FROMOD 26
2.3.3.2. SOLMOD 27

3. RESULTS 28

3.1. Transpiration Limitations 29
3.2. Steady Flap Case 30
3.3. Plate Case 34
3.4. AGARD Wing 54
3.5. Mesh Sensitivity 66
3.6. Plate with 0.5 Generalized Displacements 70

4. CONCLUSIONS AND RECOMMENDATIONS 74

4.1. Conclusions 74
4.2. Recommendations 75

BIBLIOGRAPHY 77

APPENDIX--ADDITIONAL DATA 79

LIST OF TABLES

Table Page

3.1. Generalized Forces for Mach 0.3 42

3.2. Generalized Forces for Mach 0.95 48

3.3. Generalized Forces for Mach 3.0 52

3.4. Generalized Forces for Old and New Meshes 69

3.5. Summary of Results for 0.5 Generalized Displacement Plate 71

LIST OF FIGURES

Figure Page

2.1. Transpiration Implementation 18

2.2. Method of Surface Deflection Flowchart 25

3.1. NACA 0012 Airfoil with Deflected Flap 31

3.2. NACA 0012 Surface Pressure Results From Panel Code 32

3.3. NACA 0012 Surface Pressures from Panel Code and from Raj 33

3.4. Surface Mesh for Plate Case 35

3.5. Six Vibrational Modes for Plate Case 37

3.6. Deflected Plate Surface 38

3.7. Actual Pressure Contours, Mach 0.3 39

3.8. Pressure Contours Using Transpiration, Mach 0.3 39

3.9. Pressure Cut Stations 40

3.10. Pressure Profiles, Mach 0.3 41

3.11. Actual Pressure Contours, Mach 0.95 43

3.12. Pressure Contours Using Transpiration, Mach 0.95 43

3.13. Pressure Profiles, Mach 0.95 45

3.14. Mach Profiles, Mach 0.95 47

3.15. Actual Pressure Contours, Mach 3.0 49

3.16. Pressure Contours Using Transpiration, Mach 3.0 49

Figure Page

3.17. Pressure Profiles, Mach 3.0 51

3.18. Residual Convergence 53

3.19. AGARD Wing 54

3.20. Deflected AGARD Wing 55

3.21. Actual Pressure Contours, Mach 0.99 56

3.22. Pressure Contours Using Transpiration, Mach 0.99 56

3.23. Pressure Profiles, Mach 0.99 58

3.24. Actual Pressure Contours, Mach 1.141 59

3.25. Pressure Contours Using Transpiration, Mach 1.141 60

3.26. Pressure Profiles, Mach 1.141 61

3.27. Actual Pressure Contours, Mach 2.0 62

3.28. Pressure Contours Using Transpiration, Mach 2.0 63

3.29. Pressure Profiles, Mach 2.0 64

3.30. Original Plate Mesh 66

3.31. Pressure Profiles for New and Old Plate Cases 68

3.32. Deflected Plate, 0.5 Generalized Displacements 70

3.33. Time History of Generalized Forces 72

3.34. Average Percent Error in Generalized Forces 73

A.1. AGARD Wing 80

A.2. Deflected AGARD Wing, 2.63 Units Bending and 0.33 Units Torsion 80

A.3. Actual Pressure Contours, Mach 0.678 81

A.4. Pressure Contours Using Transpiration, Mach 0.678 81

Figure Page

A.5. Pressure Profiles, Mach 0.678 82

A.6. Actual Pressure Contours, Mach 0.99 83

A.7. Pressure Contours Using Transpiration, Mach 0.99 83

A.8. Pressure Profiles, Mach 0.99 84

A.9. Actual Pressure Contours, Mach 2.0 85

A.10. Pressure Contours Using Transpiration, Mach 2.0 85

A.11. Pressure Profiles, Mach 2.0 86

CHAPTER 1

INTRODUCTION

1.1. Background

Ever increasing technological advancements have lead to the development of aircraft that operate at greater and greater velocities. Today, aircraft that are designed and manufactured to perform near and above sonic speeds are much more common. For example, it is typical for aircraft, from military fighter planes to modern airliners, to have cruise speeds in the transonic range. In the design and performance analysis of these vehicles, it is important to study their aeroelastic characteristics. Even for vehicles traveling at subsonic speeds, the flow can cause a body deformation in the structure, which in turn will affect the flow solution. The coupling between fluid and structural forces can induce unstable oscillations. Therefore, it is important to accurately predict a vehicle's flutter boundaries, since inaccurate predictions could result in vehicle failure.

Often in modern three-dimensional aeroelastic analysis, a flow solver is employed in conjunction with a structural solver. The solutions of the flow field and the surface oscillation are performed simultaneously. Many flow solvers used today employ a grid

and the surrounding flowfield. Movement of the body under investigation due to the surface loads must be accounted for. This requires that either the surface grid be modified to match the body deflection, or that the deflection be simulated by some means. One possibility for simulating the deflection is to modify the surface normals at their original locations. Thus, to the flow field, the surface appears to have an altered form. This concept is known as the transpiration boundary condition and is the focus of this study.

1.2. Problem Statement

In unsteady aeroelastic analysis, the position and orientation of the surface under investigation are a function of time. In order for the solution to be determined accurately, the surface deformation must be represented. The most direct representation would appear to be regenerating the computational grid. However, in a time stepping approach, this would require that the grid be regenerated at each time step, since the surface will change with every time step. Using this procedure with present computer capabilities, a solution for a single set of parameters using grid regeneration could be on the order of weeks.

The present study uses an integrated computer code called STARS (STructural Analysis RoutineS) that is capable of performing the steady and unsteady fluid and structural analysis of flight vehicles that are required for determining flutter boundaries. The Euler based flow solver is a recent addition to the code and is capable of simulating

three-dimensional compressible inviscid flows. It uses finite element techniques with unstructured adapted meshes of tetrahedral elements. Flow solutions using this code are performed in a time-marching fashion. Thus, in unsteady aeroelastic applications, the surface deformation must be represented at each time step. This is accomplished using the transpiration boundary condition in which the original computational domain remains unaltered. The surface deflections are simulated by applying the deflected body normals at the undeflected body location, thus reducing the time required for determining flutter boundaries.

1.3. Motivation for the Study

In any field of study it is important to search for ways of improving solution characteristics, whether it be solution accuracy, expediency, or cost efficiency. A coupled fluid-structure time marching solution can be highly time consuming. For example, on present high-speed workstations, the calculation of a single fluid-structure transient on a three-dimensional aircraft configuration using the Euler equations may require over 100 cpu hours. Therefore, it is highly desirable to develop means of reducing the required computational time while maintaining solution accuracy. Advancements in computer technology are continually assisting in this task. However, faster computers are generally more expensive, so what is gained in speed may be lost in cost. By introducing

new concepts in lieu of or in conjunction with existing methods, vast improvements in solution characteristics can often be made without significantly adverse effects.

Considering the time required to generate a single domain mesh for a flow solution, it seems highly impractical to rediscretize the computational domain at each time step. One alternative to this rediscretization was presented by Batina (1989) where he used a dynamic mesh algorithm that models a triangulated mesh as a spring network. Each edge of each triangle in the mesh is modeled by a spring whose stiffness for any edge i-j is inversely proportional to the length of the edge.

In this algorithm, the grid points on the outer boundary of the mesh are fixed and a predictor-corrector procedure that iteratively solves the static equilibrium equations in the x- and y-directions at each time step is used to determine the displacements δ_{xi} and δ_{yi} at each interior node i. The method predicts displacements according to

$$\tilde{\delta}_{x_i} = 2\delta^{n}_{x_i} - \delta^{n-1}_{x_i}$$

$$\tilde{\delta}_{y_i} = 2\delta^{n}_{y_i} - \delta^{n-1}_{y_i}$$

It then corrects the displacements using several Jacobi iterations of the static equilibrium equations using

$$\delta^{n+1}_{x_i} = \frac{\sum k_m \tilde{\delta}_{x_m}}{\sum k_m}$$

$$\delta_{y_i}^{n+1} = \frac{\sum k_m \tilde{\delta}_{y_m}}{\sum k_m}$$

where k_m is the spring stiffness, and the summations are over all edges of the triangles that have node i as an endpoint. Finally, the new nodal coordinates are given by

$$x_i^{n+1} = x_i^n + \delta_{x_i}^{n+1}$$

$$y_i^{n+1} = y_i^n + \delta_{y_i}^{n+1}$$

This algorithm was found to produce good results when used in unsteady pitching and plunging studies, and also in the prediction of flutter boundaries. However, it is necessary to perform the displacement calculations at each node for every time step in both coordinate directions. Additional computations will be required if the algorithm is extended to three-dimensions.

This number of calculations can be significantly reduced if the surface deflection can be simulated without having to alter the existing grid. One way to simulate body deflection is to apply a transpiration boundary condition at the surface. This is essentially done by rotating the body normals so that the new normals are in the same directions they would be in if the body had actually deflected. Thus the original body grid remains unaffected throughout the flutter investigation.

Transpiration has been used effectively in simulating surface deformations in full potential solutions and steady and unsteady rigid-body applications in Euler equations. It

is the purpose of this study to show the extent to which the transpiration boundary condition may be used in unsteady aeroelastic problems.

1.4. Rationale

When the transpiration boundary condition is employed, there is potential for great savings in time requirements. However, an expedient solution is useless if its accuracy is questionable. Therefore, showing the extent to which the transpiration boundary condition is valid will allow flutter investigations to be made much more quickly and with confidence in results when inside the transpiration limits.

1.5. Flutter Analysis

Pertaining to aerodynamics, flutter is the divergent oscillation of a surface resulting from a coupling between structural and fluid forces. The prediction of flutter boundaries has been the subject of a great deal of studies. Methods that have been used in many recent studies include full potential and Euler methods. Both methods have proven effective in many flutter investigations

Full potential methods offer accurate solutions in a wide range of applications with relatively low computational costs. As with Euler methods, there is the assumption of

inviscid flow. However, since these methods use an approximation of the Euler equations, they require further assumptions. One assumption in the development of the full potential equation is irrotational flow, which in most cases is a reasonable solution. These equations also do not allow for entropy changes across shocks. Thus, the existence of shocks, even in subsonic flow, will introduce inaccuracy to the solution.

Euler methods produce a higher order, more accurate solution than the full potential methods. They are capable of accounting for viscous and entropy effects, therefore they can be used for studies of a much wider variety than the full potential methods, such as at high Mach numbers and with strong shocks. One drawback with these methods is that they are more computationally intensive. However, with ever increasing advancements in computer technology, these methods are becoming much more computationally affordable and widespread.

1.6. Literature Review

1.6.1. Transpiration Concept

In 1958, M. J. Lighthill presented four alternatives for the treatment of displacement thickness. One of these alternatives was termed "method of equivalent sources". The idea used in this method has today developed into what is known as transpiration. Rather than thickening an airfoil to account for the boundary layer, an

equivalent surface distribution of sources is used to "simulate" a thicker airfoil. This is done by modifying the normal velocity just outside the boundary layer to include additional outflow due to the boundary layer.

1.6.2. Transpiration in Full Potential Studies

One early study in which transpiration was used in conjunction with a flutter solution was performed by Sankar, Malone, & Tassa [1981]. The study was performed using a full potential method. Although not explicitly stated, transpiration was used in "simulating" the first order bending of an oscillating rectangular wing in subsonic flow. This was done by applying the zero normal velocity boundary condition for the deflected surface at the undeflected wing position. Computations were also performed by applying the boundary condition at the actual surface. The authors reported making both computations to ensure that the differences were small, however, results were only presented for the transpiration solutions.

Lift, moment, and phase results were presented for the transpiration computations at a Mach number of 0.24 and were compared to experiment and Kernel function solutions. It was concluded that the results compared reasonably well. It was noted that the simulated results more closely resembled the Kernel function than the experiment. This was attributed to neglecting viscous effects and the fact that the experiment used a

5% thick circular arc airfoil. Furthermore, it was concluded that the simulation accurately and reliably predicts unsteady subsonic potential flow.

This transpiration boundary condition was further used in a study of a fighter wing in transonic flow [Malone, Sankar, & Sotomayer, 1984]. The study incorporated transpiration with the full potential equations to estimate the 1st harmonic, real and imaginary components of unsteady surface pressures at eight different stations on an F-5 fighter wing. Computed and experimental results were presented for three transonic Mach numbers (0.8, 0.9, and 0.95). It was concluded for this study that the results correlated reasonably well. It was further concluded that this method could be used in studying flutter behavior of fighter type wings at transonic speeds.

Based on these validating results, Malone & Sankar [1985] used transpiration with full potential equations to study the unsteady pitching oscillation for the RAE wing-body model in transonic flow (Mach = 0.8). Unsteady surface pressure results were presented, however, no experimental data was available for comparison.

Then, in 1986, a study was performed exclusively to compare results from a full potential method using the exact boundary condition and the transpiration boundary condition [Sankar, Ruo, & Malone]. Results were presented for a NACA 64A006 airfoil with an oscillating trailing edge flap, a large aspect ratio wing in independent pitching and plunging, a plunging fighter wing, and a steady rectangular wing.

The NACA 64A006 results were computed at a freestream Mach number of 0.875. The results showed that pressure distributions were within plottable accuracy of one another, and that integrated loads were within 10% of each other. The first harmonic out

of phase component of the surface pressure distribution was also determined for the flap case and compared to experiment. Results for both exact and transpiration approaches and experimental data were found to be in close agreement, the only appreciable difference being near the sonic line.

The next configuration in the study was a large aspect ratio wing. Results were presented for three plunge velocities (corresponding to 1, 5, and 10 degrees steady angle of attack) at Mach = 0.77. At 1 degree, the results proved to be nearly identical. At the larger plunge values, the results were not as close but still very good (within 10%). Pitching results using the transpiration approach were also computed at Mach = 0.66 and compared to results from a vortex lattice method (for pitching rates of 1, 5, and 10 degrees/second). In each case, the transpiration prediction was larger than that of the vortex lattice method, the worst case being over 30%. However, the vortex lattice method does not consider airfoil thickness effects and therefore underpredicts the airloads.

Surface pressure distributions at four span locations were present for a Mach 0.95 fighter wing undergoing constant plunging motion (1.5 degrees effective plunge velocity) Transpiration and exact approaches were compared with experiment. Both approaches were found to closely match experiment, except for slightly smeared shocks predicted by transpiration. This was suspected to be due to the use of a somewhat coarser grid in the transpiration case.

The final study used transpiration to simulate steady viscous effects of a rectangular wing in transonic flow. The wing was analyzed at an angle of attack of 2.0 degrees and a Mach number of 0.8. Surface pressure distributions were calculated, with

and without viscous corrections, and compared with experiment. Solution accuracy showed improvement when transpiration was used for viscous corrections.

It was concluded from this study that for small amplitude motions, as in aeroelastic applications, the transpiration boundary condition provides accurate results. Furthermore, the authors cited a considerable savings in coding effort and memory requirements when using the transpiration boundary condition.

1.6.3. Transpiration in Euler Studies

The transpiration boundary condition was used with the unsteady Euler equations in a study of transonic flow past a fighter wing by Sankar, Malone, & Schuster [1987]. The pitch oscillation of the fighter wing was accounted for by changing the boundary condition and leaving the original surface unmodified. In-phase and out-of-phase components of the surface pressure distribution were calculated at four span locations and compared with experiment. The fighter wing Mach number was 0.8, and the pitching amplitude was 0.113 degrees at 40 Hz (zero mean angle of attack). Slightly higher suction levels were predicted by the Euler solver for the in-phase component near the leading edge. However, overall experimental and calculated results were found to be in very good agreement. It was concluded by the authors that the unsteady Euler solver with transpiration was robust enough and accurate enough to be used in aeroelastic studies.

Transpiration was again used in the unsteady Euler investigation of two pitching wings; a transonic (Mach 0.82) transport-type wing and a subsonic (Mach 0.7) rectangular wing [Ruo & Sankar, 1988]. The transport-type wing was the Lockheed-Air Force-NASA-NLR (LANN) wing. Its oscillating pitch amplitude was 0.6 degrees at a frequency of 24 Hz. The rectangular wing's oscillating pitch amplitude was 2 degrees at a frequency of 10 Hz.

In-phase and out-of-phase components of the surface pressures were presented for calculated and experimental results at four span locations for each wing. For the LANN wing, there are significant differences in results at some locations. However, according to the authors, the experimental data at many locations is not considered reliable for this wing. When the unreliable data is ignored, results for both components show good agreement. For the rectangular wing, calculated and experimental results agree everywhere except near the wing tip for the in-phase component, which may be due to viscous effects.

Midspan unsteady pressures were compared for both exact and transpiration methods. For the LANN wing, a steeper variation of the pressure near shock waves was predicted by transpiration, but away from shocks, the results were very similar. For the rectangular wing, almost identical results were predicted by both methods.

For this study, it was concluded that the overall agreement of results was good. However, the issue of which boundary condition was more favorable for small-amplitude motions was inconclusive.

More recently, a study was performed using transpiration with an Euler method to simulate control surface deflections [Raj & Harris, 1993]. The study included the trailing-edge flap deflections for a NACA 0012 airfoil and for an arrow-wing body configuration. Actual and simulated surface pressures were presented for the NACA 0012 airfoil with a 10 degree flap deflection at Mach numbers 0.6 and 0.9. For both Mach numbers, the transpiration method produced results that were in very good agreement with actual results.

The arrow-wing body configuration was analyzed using both a coarse and a fine grid, the fine grid having higher resolution around the wing. Simulated results were computed and compared with experimental data. Surface pressure distributions were presented at three span locations for 0, 4, and 8 degrees angle of attack with and without a flap deflection of 8.3 degrees. No experimental data was presented for the zero degree case with no flap deflection, but results for the fine and the coarse grids were in close agreement. Results from both grids matched well with experimental data for flap deflection at zero angle of attack.

Some noticeable differences between computed and experimental results can be seen for the outermost station in the 4-degree angle of attack case, while there is better agreement at the inner stations. However, these differences are most likely due to limitations of Euler equations, such as neglecting viscous effects, rather than transpiration. Also, the finer grid appears to produce data near the leading edge that is slightly closer to the experimental.

In the 8-degree angle of attack case, results for the innermost station are very close. Differences are seen at the middle station, but they are not a result of transpiration. The differences are a result of Euler computations producing attached flow where experimental data suggests flow separation at the leading edge. The outermost station results are not as good as the innermost, but results there are comparable.

Experimental and simulated lift and pitching-moment coefficients were also compared for the arrow-wing body case. Results were presented for 0, 8.3, and 17.7 degree trailing-edge flap deflections at Mach 0.85. For each flap deflection, the simulated lift and pitching moment results were in very close agreement.

From this study, the authors concluded that transpiration boundary condition was effective in estimating the changes in aerodynamic forces, moments and surface loading due to control-surface deflections, assuming that the Euler equations are capable of modeling the flow field. It was noted that transpiration was not suitable for simulating configurations that may produce geometric gaps.

1.7. Objectives of the Present Study

The STARS group, for which this study was performed, has recently added an unsteady Euler flow solver that uses transpiration to simulate surface deflections and deformations. The primary objective of this research is to employ this new code over a

wide Mach number range in the analysis of unsteady aeroelastic problems, and to document the extent to which the transpiration boundary condition is effective.

It is evident that the transpiration boundary condition can be used effectively to a large extent in applications of relatively small displacements. It is also apparent that this boundary condition can be an effective tool in aeroelastic investigations. However, it is important to be aware of what circumstances will cause the boundary condition to introduce appreciable inaccuracies. Therefore, this study will present the rationale for when and why the transpiration boundary condition will give inaccurate results and to perform investigations to support the rationale.

A secondary objective of this study is to determine how much influence grid resolution has on any given solution. This is a direct result of the primary objective because it is important to distinguish between inaccuracies due to transpiration and mere differences due to mesh sensitivity.

CHAPTER 2

METHODOLOGY

In this research effort, the transpiration concept was applied to various steady and unsteady cases. The preliminary results were obtain using a steady panel code that was modified to use transpiration for steady deflections. The majority of the results obtained from this study used an Euler based code that employs the transpiration boundary condition in steady and unsteady surface deflections and deformations. Computer codes were also developed in this study to produce actual surface deflections for use with the Euler code.

2.1. Transpiration Development

The idea of transpiration was first developed by Lighthill [1958] as a method of equivalent sources. Lighthill modified the normal velocity just outside the boundary layer of an airfoil through an equivalent surface distribution of sources to "simulate" a thicker airfoil. In this way, the effect of a boundary layer is present in the solution without

physical representation of a true boundary layer. Applied mathematically, the normal velocity w is

$$w = \int_0^z \frac{\partial w}{\partial z} dz = -\int_0^z \frac{\partial u}{\partial x} dz = -\frac{dU}{dx} z + \frac{\partial}{\partial x} \int_0^z (U - u) dz = -\frac{dU}{dx} z + \frac{d}{dx} \int_0^\infty (U - u) dz.$$

where z is the distance from the surface and u is the x component of velocity, which takes the value U just outside the boundary layer. The first term is the original, unmodified normal velocity. The second term represents the normal velocity contribution from the boundary layer. Thus, the flow field "sees" the effects of a boundary layer that is not physically present.

In this study, transpiration is applied as a boundary condition such that geometric changes and motions are simulated through surface transpiration. The unsteady boundary condition states that the velocity component normal to the body surface must equal the velocity of the body surface,

$$\mathbf{V} \cdot \mathbf{n} = \mathbf{V}_{\mathbf{body}} \cdot \mathbf{n}$$

thus there can be no flow through the surface. With transpiration, this done by adding a velocity component normal to the tangential velocity so that the resultant velocity is at some angle to the original surface, as shown in Figure 2.1.

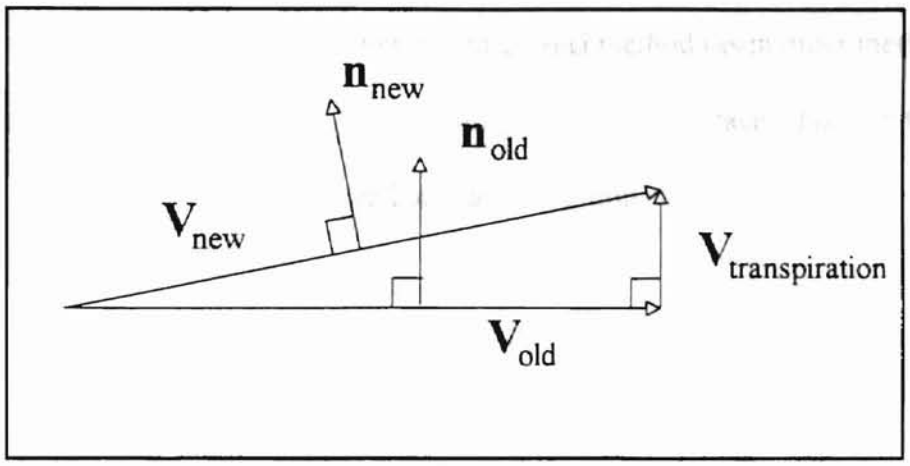

Figure 2.1. Transpiration Implementation

This velocity is then taken as the new tangential velocity. Thus the solution is performed on a seemingly different surface.

2.2. Steady Panel Methods

In general, panel methods use a distribution of singularity elements (e.g. sources and vortices) over a solution boundary to satisfy the solution boundary conditions. This is accomplished by using discrete singularity "panels" over the body surface (and possibly other areas, such as the wake). Combining the velocity potential of each singularity element with that of the freestream, the continuity equation is solved with the proper boundary conditions to give a unique solution for the velocity potential.

One of the conditions that is imposed in a panel method (as in other methods) is flow tangency; that is, there can be no flow through the body surface. Thus, in the solution of a steady panel problem, the boundary condition is

$$\mathbf{V} \cdot \mathbf{n} = 0$$

must be satisfied on each panel, where **n** is the panel normal. To apply transpiration to a panel method, essentially all that needs to be done is to rotate either the panel angle or the panel normal.

The first investigation that was performed used transpiration with a 2D, steady panel code. This code, written by Arena [1993], employs the Smith-Hess panel method. Results were computed for an NACA 0012 airfoil with an actual and a simulated trailing edge flap deflection. In the actual solution, the coordinates of the original airfoil were changed at the flap location to create a 10 degree flap deflection. For the transpiration solution, the angle of each panel in the region of the flap is modified with respect to the free stream in the calculation of the influence coefficients.

2.3. STARS Code

The computer code system used to generate the majority of the comparison data for this study was an extension of the original STARS (STructural Analysis RoutineS)

computer program. STARS is an integrated FORTRAN code for the multidisciplinary analysis of flight vehicles (STARS users manual, 1995). Features of the system include structural analysis, computational fluid dynamics, heat transfer, and aeroservoelastic modules. The most recent version was written under the direction of K. K. Gupta (1995) at the NASA Dryden Flight Research Center primarily to support NASA flight operation, and research and development projects. Until recently, STARS used linearized aerodynamic theory for the prediction of the unsteady flowfields interacting with the elastic motion of an aircraft. This technique produces adequate results for a wide range of problems but has some significant limitations, such as only producing valid results for small perturbation flows. The technique also assumes simple harmonic motion which hinders studies of arbitrary or transient motions.

Due to these limitations, an unsteady Euler CFD module was added which uses transpiration to simulate body surface motion. However, this addition was limited to simulations of single-degree-of-freedom, rigid body, simple harmonic motions. Since a primary responsibility of the STARS group was to calculate aeroelastic effects in support of fight test operations, the program was modified by the STARS group (Gupta, 1995) at NASA Dryden to allow calculation of arbitrary motion and aeroelastic effects.

The code uses finite element analysis to derive the frequencies and mode shapes of the structure. The modal superposition method is then used for the dynamic structural response analysis. The recent addition to the code is a module that enables the computation of unsteady aerodynamic forces employing the finite element-based structural

and computational fluid dynamics computations. This code was validated with theoretical and experimental results.

2.3.1. Flow Solver

The flow solver portion of STARS is an Euler based code capable of simulating three dimensional compressible inviscid flows. It uses finite element techniques with unstructured adapted meshes of tetrahedral elements. The mesh is generated using an advancing front technique, which has the advantages of application to arbitrary shapes, varying grid density in the domain, and the ability of adaptive mesh generation in accordance with solution trend.

The flow solver is comprised of different modules that perform mesh generation and flow solution. The five main modules are as follows:

- SURFACE: generates the two dimensional front
- VOLUME: generates the three-dimensional tetrahedral mesh
- SETBND: sets the boundary conditions on the domain
- EULER_STEADY: performs the steady Euler flow solution
- EULER_UNSTEADY: performs the unsteady Euler flow solution

There is also mesh geometry and flow visualization through the XPLOT and ZPLOT modules of the STARS system. Adaptive mesh techniques are also possible through the module REMESH.

To begin a flow solution study, the user must define the curve components, surface components, curve segments, and surface regions that are necessary to describe the geometry of the problem. The user must also define the background mesh and the nodal spacing parameters. Taking these definitions as inputs, the code automatically generates the surface and volume meshes using the advancing front technique.

The user must then define the boundary condition types for the curves and surfaces to be used by the preprocessor. Finally, the user must create a namelist file that assigns flow conditions and coefficients. The code then takes all of the user input files, plus the files it generates in constructing the mesh and preprocessing the flow information, and performs the steady flow solution. The unsteady flow solution is then performed using the steady flow solution as the initial condition.

2.3.2. Aeroelastic and Aeroservoelastic Solver

The structural solver performs nonlinear, CFD-based aeroelastic and aeroservoelastic analysis. The structural modeling uses a finite element method, thus creating a unified approach using finite element analysis for both the flow and the structural solution. The natural frequencies (ω) and modes (ϕ) are computed by solving

$$M\ddot{u} + Ku = 0$$

where M and K are the inertial and stiffness matrices, respectively, and u is the displacement vector. The steady-state Euler solution is then performed using either an explicit or a quasi-implicit, local time stepping solution procedure that employs a residual smoothing strategy. The equation of motion in the frequency domain is

$$\hat{M}\ddot{q} + \hat{C}\dot{q} + \hat{K}q + \hat{f}_a(t) + \hat{f}_I(t) = 0$$

where

$\hat{M}$	=	inertial matrix ($=\Phi^T M\Phi$), and similarly
$\hat{K}, \hat{C}$	=	stiffness and damping matrices
q	=	displacement vector ($=\Phi^T u$)
$\hat{f}_a(t)$	=	aerodynamic (CFD) load vector ($=\Phi_a^T pA$), where p is the Euler pressure, A the appropriate surface area, and Φ_a the modal vector pertaining to aerodynamic grid points interpolated from relevant structural nodes

and

$\hat{f}_I(t)$	=	impulse force vector ($=\Phi^T f_I$)

where f_I is a number of modes input by the user. The state-space form of the equation is

$$\dot{X} = AX + b_a(t) + b_l(t)$$

where

$$X = \begin{bmatrix} q \\ \dot{q} \end{bmatrix}$$

$$A = \begin{bmatrix} 0 & I \\ -\hat{M}^{-1}\hat{K} & -\hat{M}^{-1}\hat{C} \end{bmatrix}$$

$$b_a(t) = \begin{bmatrix} 0 \\ -\hat{M}^{-1}\hat{f}_a(t) \end{bmatrix}$$

$$b_l(t) = \begin{bmatrix} 0 \\ -\hat{M}^{-1}\hat{f}_l(t) \end{bmatrix}$$

and a time response solution of the state-space equation in an interval Δt (= t_{n-1} - t_n) is obtained as

$$X_{n+1} = e^{A\Delta t}X_n + A^{-1}\left[e^{A\Delta t} - I\right]\left[b_a(t_n) + b_l(t_n)\right]$$

The structural deformations u and velocities $\dot{u}$ are then computed and used by the CFD code to change the velocity boundary conditions at the solid boundary. Then a one-step Euler solution using a global time-stepping scheme is performed and the process is repeated for the required number of steps.

2.3.3. Code Modifications

The original unsteady Euler code that was used in this investigation performs surface deflections using transpiration only. If comparisons of these transpiration results

were to be made against actual deflection results, it would be necessary to produce a method of generating a deformed surface mesh. Essentially, the problem reduces to assembling a code that modifies a given surface as desired and a code for calculating the correct normals. Once the deflected surface is obtained with the proper normals, the steady Euler code can be used to perform the flow solution.

The two codes generated to complete the process for obtaining the actual solution were FROMOD and SOLMOD. A flow chart depicting the process is presented in Figure 2.3.

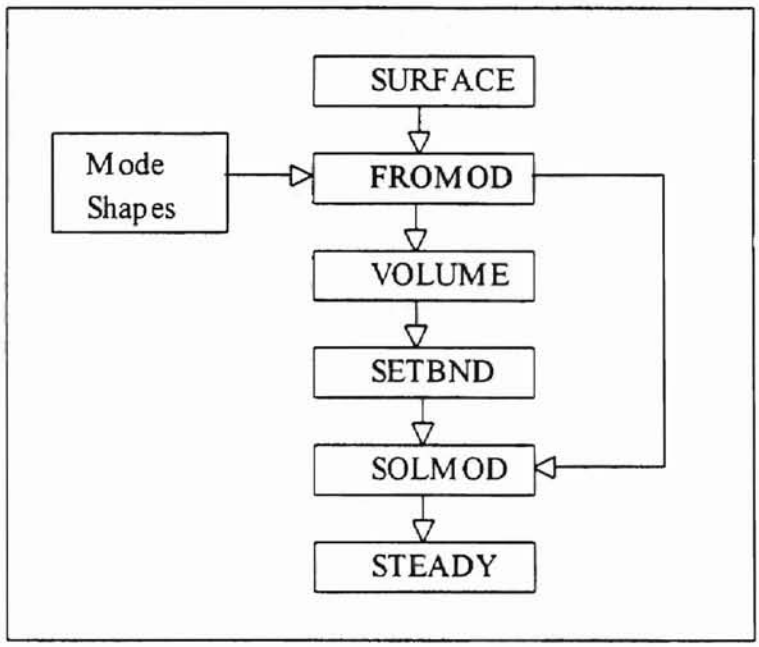

Figure 2.2. Method of Surface Deflection Flowchart

The flow chart shows that the original surface mesh does not need to be modified to deform the surface. A discussion of each code is presented in the follow sections.

2.3.3.1. FROMOD

The three basic components required for performing surface deflection are the original, unmodified mesh, the mode shapes of the different modes, and scaling factors specifying the generalized displacements. The unmodified mesh can be obtained by generating the mesh on the original surface. The mode shapes are obtained from the finite element structural solver. The final requirement is a set generalized displacements, which is provided by the user.

The original surface is altered by displacing each node point in each coordinate direction, x, y, and z, on the surface by an amount that is determined from the mode shapes and their generalized displacements. For example,

$$x_{new}(i) = x_{old}(i) + \Delta x(i)$$

where $\Delta x(i)$ is determined by

$$\Delta x(i) = \sum_{j=1}^{n} \Phi_a(i,j) * f_1(j)$$

where $\Phi_a(i,j)$ is an array of mode shapes

$f_1(j)$ is an array of generalized displacements, input by the user

and n is the number of modes

Essentially, FROMOD is used to generate a deformed surface mesh. It reads in the surface definition and the generalized forces and prompts the user for the modal scaling factors. Using this data, the code generates an array of nodal displacements and adds these displacements to the original nodes, as previously described. Then the code writes the new surface file. One advantage of this procedure is that the connectivity of the surface is unchanged, so it can simply be transferred from the old surface file to the new one. The final requirement is a code to calculate the normals for the deflected surface. This code is discussed in the following section.

2.3.3.2. SOLMOD

A second modification code was required to complete the process for determining actual deflection solutions. This code, called SOLMOD, was needed to calculate the surface normals for the new mesh. SOLMOD reads in the file containing the normals, corrects the normals, and then overwrites the old normals file with the new one.

The computational process for modifying the normals already existed in the Euler code because it is used in the transpiration solution. In this process, the normals at each node in the mesh are calculated using an area weighted average of surface triangulations that contain that node. Since this coding was already present, it was simply combined with the proper read and write statements to create SOLMOD.

CHAPTER 3

RESULTS

The main objective of this study was to determine the effectiveness of the transpiration boundary condition in unsteady aeroelastic applications. This was to be done by performing investigations of various geometries over a wide range of Mach numbers. By doing so, this boundary condition could be employed in the prediction of flutter boundaries. The rationale is to discuss the instances in which transpiration will introduce error into the solution, and to generate comparison data to show the effectiveness of transpiration in various applications. The following section contains a discussion of the limitations. Subsequent sections present results demonstrating the capability of transpiration.

The first set of results that is presented is for a steady, trailing edge flap deflection, as a preliminary investigation. The next two sets of results comprise the core of the research, the first being a 2 by 1 flat plate and the second being the AGARD 445.6 wing. In these cases, solutions were performed for actual deflections and compared to simulated deflections using transpiration. The final cases of the study address the issue of mesh sensitivity in computational fluid dynamic solutions.

3.1. Transpiration Limitations

The idea of transpiration is essentially to alter the boundary condition when performing a flow solution. In using transpiration, if the surface under investigation deflects, the surface normals are modified to account for the deflection. Therefore, if the deflection is small, transpiration can very accurately predict the solution. This is because the relative position of one part of the surface to another will have little effect. However, as the deflection increases, the accuracy of the transpiration solution will decrease. Since transpiration only accounts for the orientation of the normals, the effect of translation between two points on the surface will not be accounted for in the solution.

As an example of this translation problem, consider a wing that has first mode bending such that the free end is no longer in the same plane as the fixed end. When transpiration is used to simulate the bend, the normals along the wing will be altered in the wing's original position. Thus the effect that a point on the displaced end has on points elsewhere will not be completely accurate, and increasing the displacement will add to the inaccuracy.

One consequence of the translation effect is error introduced by intersecting shocks and surfaces. Consider a shock wave originating at the nose of an aircraft whose wing is oscillating in first mode bending. In the transpiration solution, the shock will

intersect the wing in its original position. However, in the actual solution the wing is displaced, thus the shock intersection will not be in the same location.

Other problems such as this could result when there is internal surface translation of the body under investigation. As mentioned, however, in cases of small deflection, such as in flutter problems, transpiration can produce very accurate results.

3.2. Steady Flap Case

In order to gain a better understanding of the transpiration concept and to perform some preliminary investigations, a panel code was modified to employ transpiration. Actual and simulated surface pressures were computed for a N0012 airfoil at Mach 0.6 and zero degree angle of attack with a steady 10 degree flap deflection. The results were obtained using a FORTRAN code written by Arena that employs the Smith-Hess panel method. Slight modifications to the code were made to obtain the transpiration results. Figure 3.1 shows the deflected flap, located at 80% of the chord.

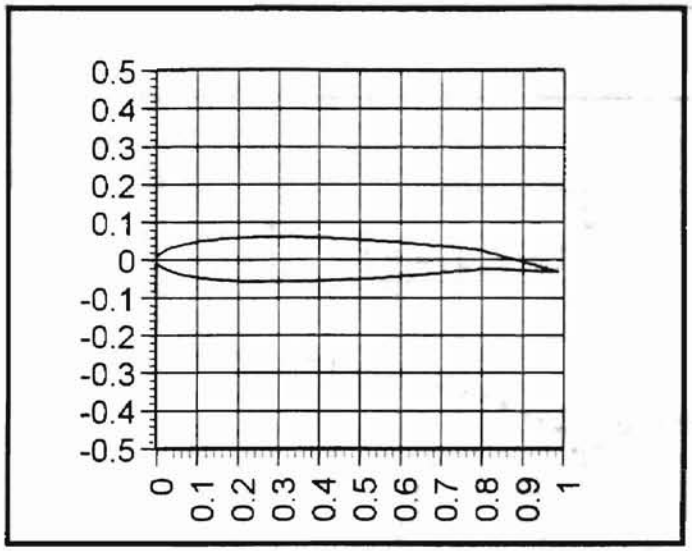

Figure 3.1. NACA 0012 Airfoil with Deflected Flap

Actual and simulated surface pressures were generated using the Smith-Hess code. These pressures were corrected for compressibility effects using Prandtl-Glauert correction. The corrected results are presented in Figure 3.2.

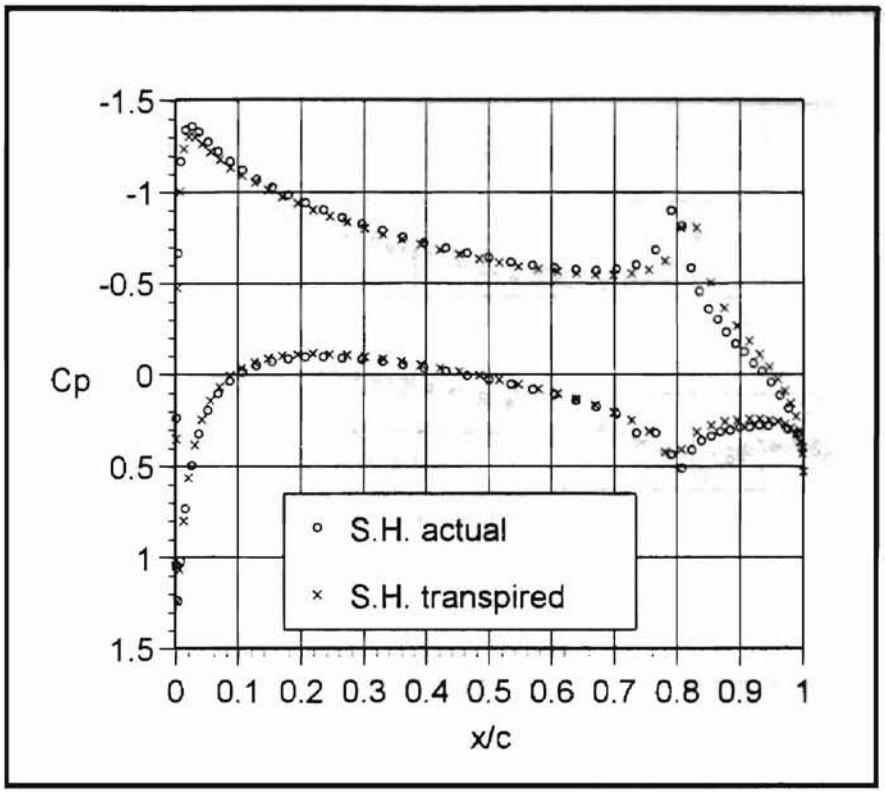

Figure 3.2. NACA 0012 Surface Pressure Results from Panel Code

It can be seen from Figure 3.2 that transpiration is very effective in simulating the flap deflection with only slight differences occurring near the flap-airfoil intersection.

This study was also performed by Raj using a steady Euler method that also employs transpiration. In that study, transpiration results were also compared against actual flap deflection results. Figure 3.3 shows the actual and transpiration simulated results obtained by both the Smith-Hess code and by Raj.

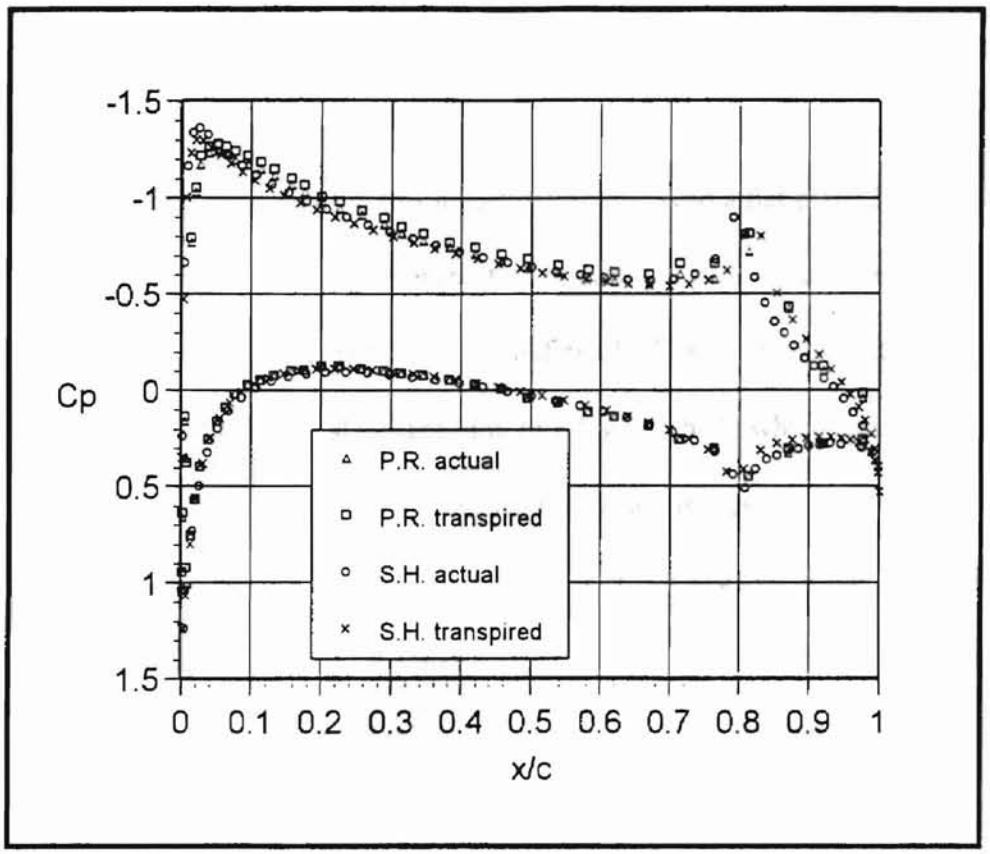

Figure 3.3. NACA 0012 Surface Pressures from Panel Code and from Raj

The results from the two studies are in very close agreement. This not only shows the effectiveness of transpiration, but it also serves as a validation of the Smith-Hess results.

Considering the magnitude of the deflection, the transpiration boundary condition appears to be very effective. This preliminary investigation suggests that transpiration has strong potential in simulating significant deflections.

3.3. Plate Case

One of the primary cases in this investigation involved a flat plate 2 units long and 1 unit wide. This type of plate is representative of configurations that have been used in well documented studies on panel flutter. As defined by Dixon , panel flutter is a self-excited oscillation of the external surface skin of a flight vehicle which results from the dynamic instability of the aerodynamic, inertia, and elastic forces of the system. Information gained from studies involving panel flutter has assisted in the pursuit for flight vehicles with increasing speeds. This investigation of panel flutter is gives a new approach to this well known problem, as it allows for flutter investigations in which the surface under consideration is never required to actually deform.

The plate used in this study was centered on a surface 4 units long by 3 units wide. This plate and the surface mesh are shown in Figure 3.4.

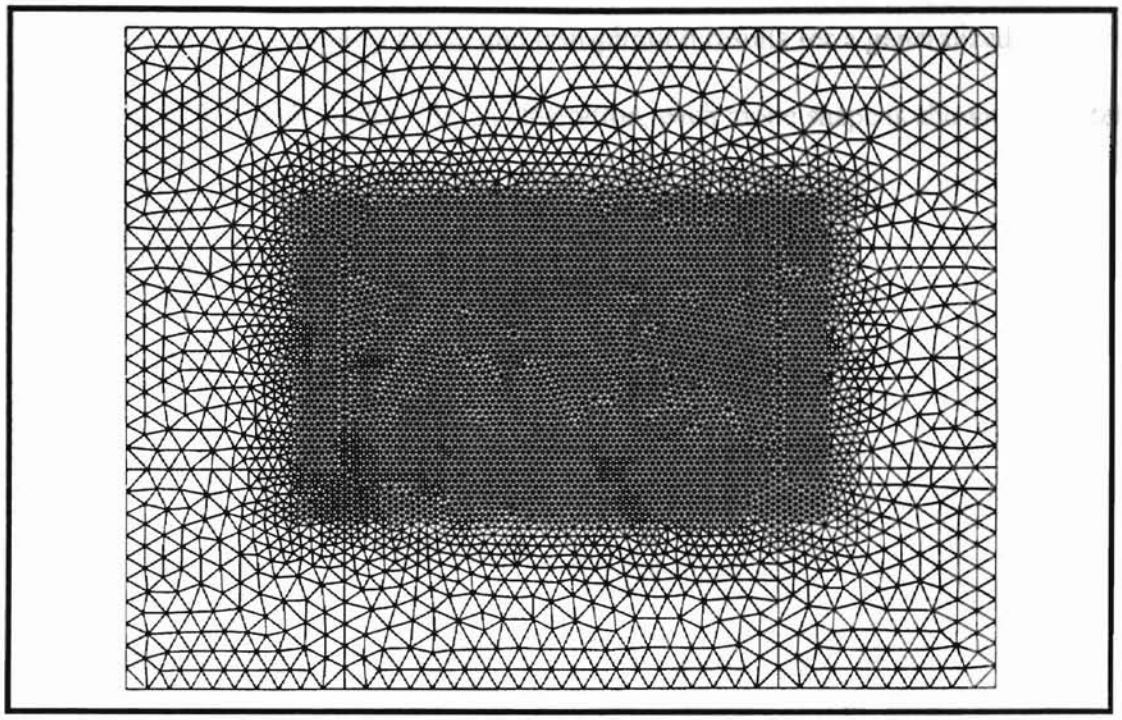

Figure 3.4. Surface Mesh for Plate Case

This figure shows that the grid resolution on and immediately around the plate is very high. This was necessary to generate a smooth flow solution over the plate. The freestream flows over the top of the plate, with both sides of the plate being at atmospheric pressure. The plate edges are pinned to the bottom surface. All surfaces are defined as walls and all edge boundaries are defined as far field. The plate is flat, but can be made to deform, as described by Section 2.3.3, or deformation can be simulated using transpiration. The deflection can be any combination of six bending modes of the plate. In plate flutter, the magnitude of deflection in each mode would not necessarily be the same. However in this study, all modal deflections were of equal magnitude for an arbitrary deflection.

The first case compares actual and transpiration results for a generalized displacement of 0.1 in all modes. As an illustration, each mode shape is shown separately in Figure 3.5.

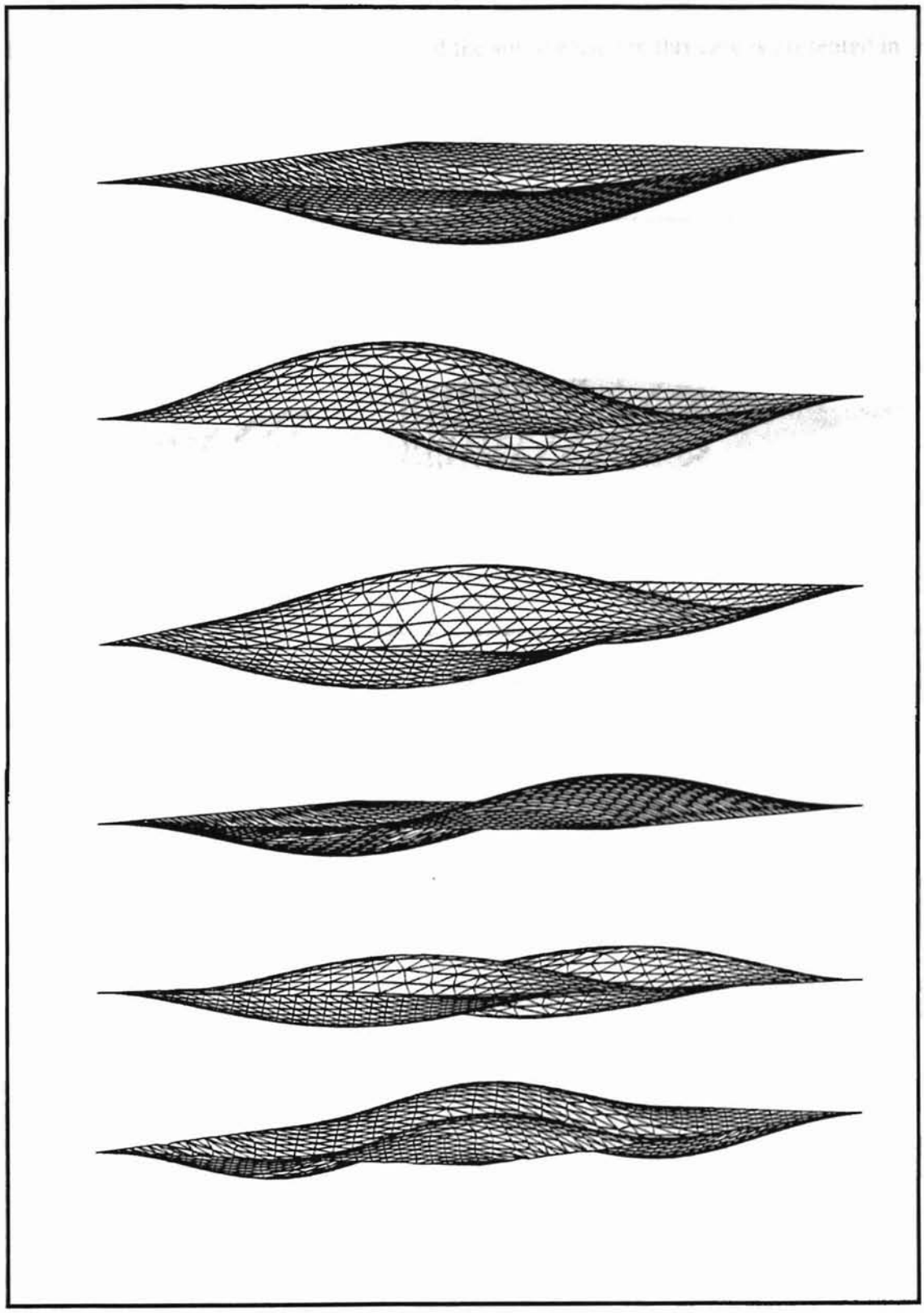

Figure 3.5. Six Vibrational Modes for Plate Case

The superposition of modes that produced the surface used in this case is presented in Figure 3.6.

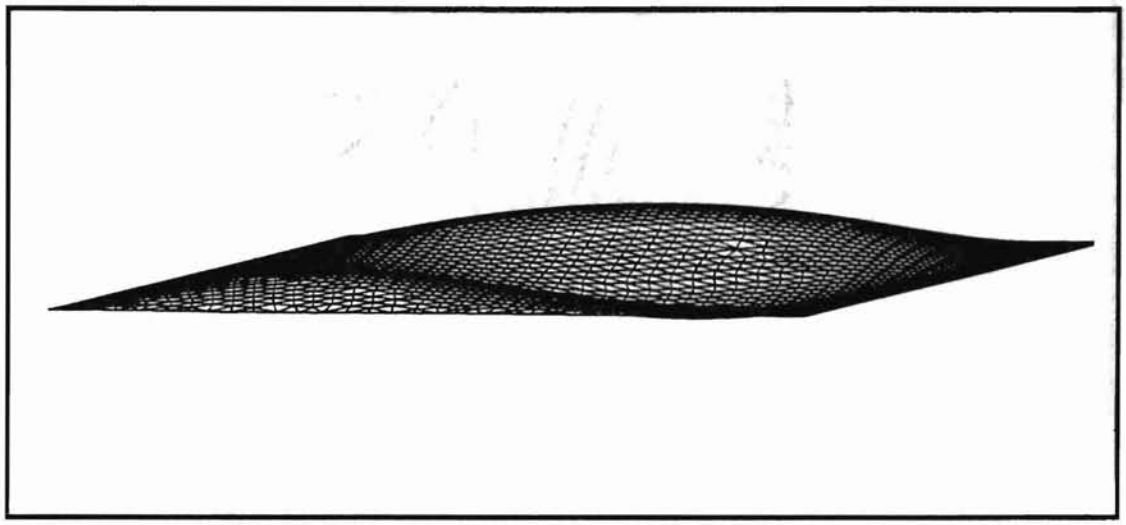

Figure 3.6. Deflected Plate Surface

The resulting deflection produces a maximum deflection that is over 7% of the width of the plate. This case was selected as an initial attempt to determine limitations of transpiration. Arbitrary deflection was used to maintain generality; 0.1 amplitudes were used to give a significant deflection. Surface pressures and generalized forces were compared for freestream Mach numbers 0.3, 0.95, and 3. In all cases, the actual and simulated surface pressures were very similar. The generalized forces were comparable, but did show some appreciable differences.

Figures 3.7 and 3.8 show actual and transpiration surface pressure contours, respectively, for the Mach 0.3 case.

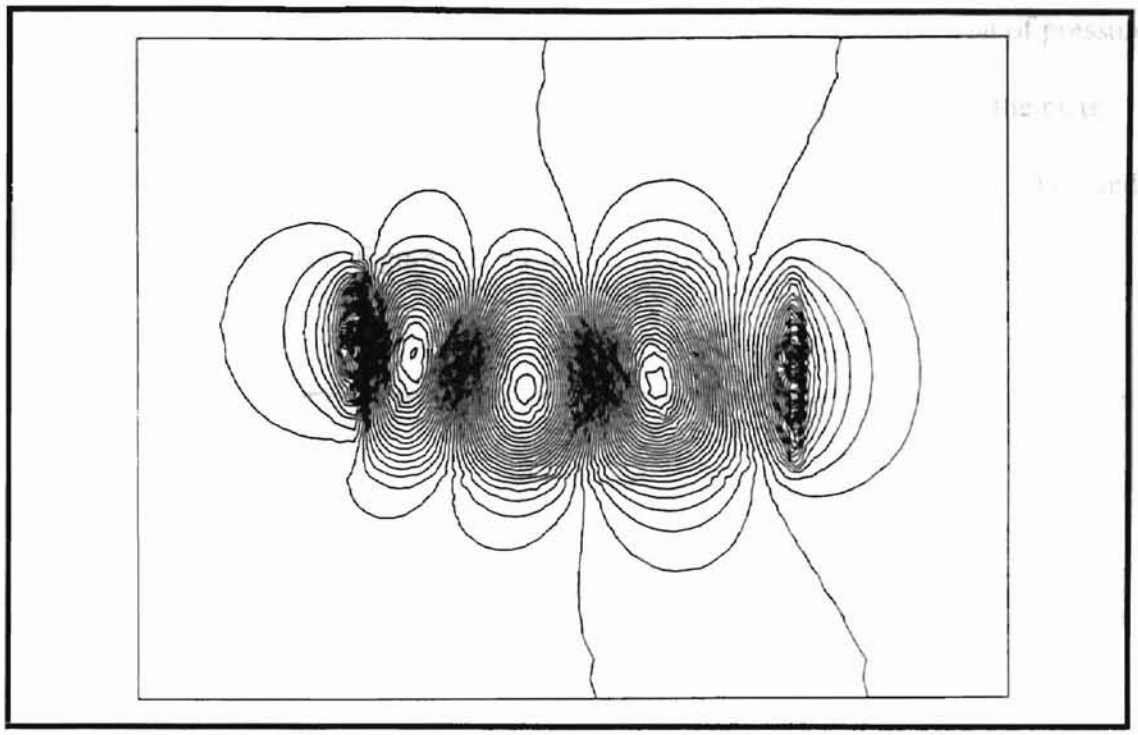

Figure 3.7. Actual Pressure Contours, Mach 0.3

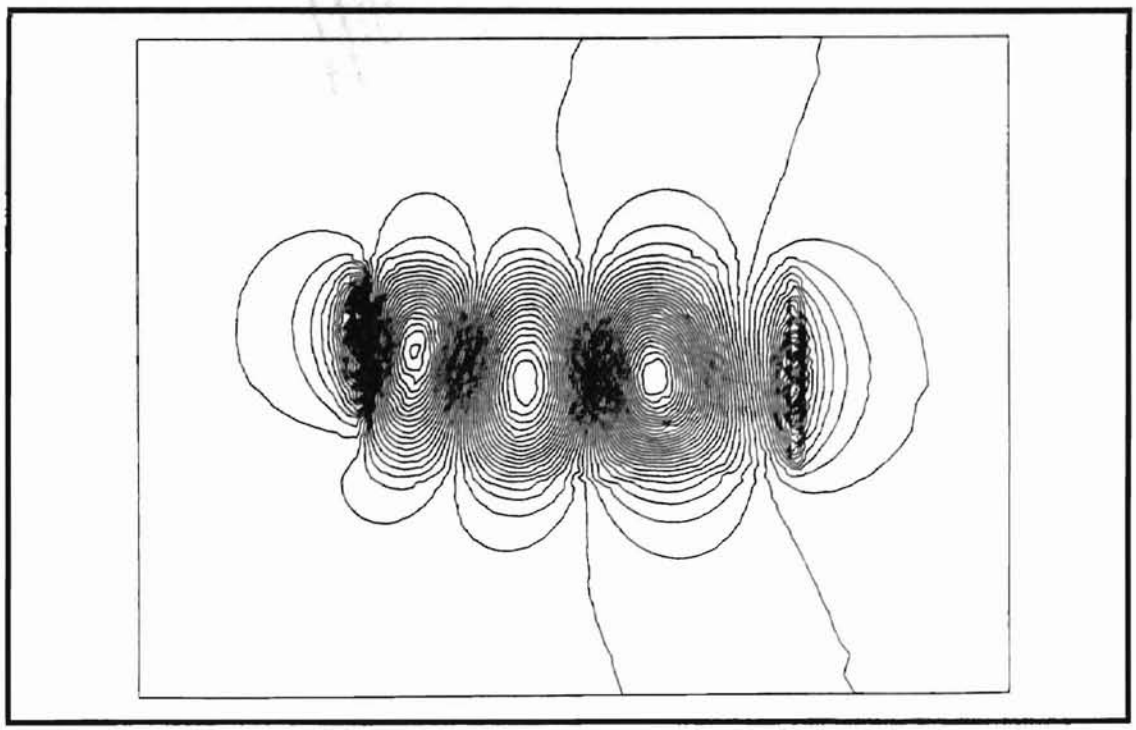

Figure 3.8. Pressure Contours Using Transpiration, Mach 0.3

It is evident that these results are very similar. For a more detailed comparison of pressure results, cross-sectional surface pressures are presented at three stations across the plate. These stations run lengthwise along the plate and are located at one-quarter, one-half, and three-quarters of the width. Figure 3.9 shows the stations across the deflected plate.

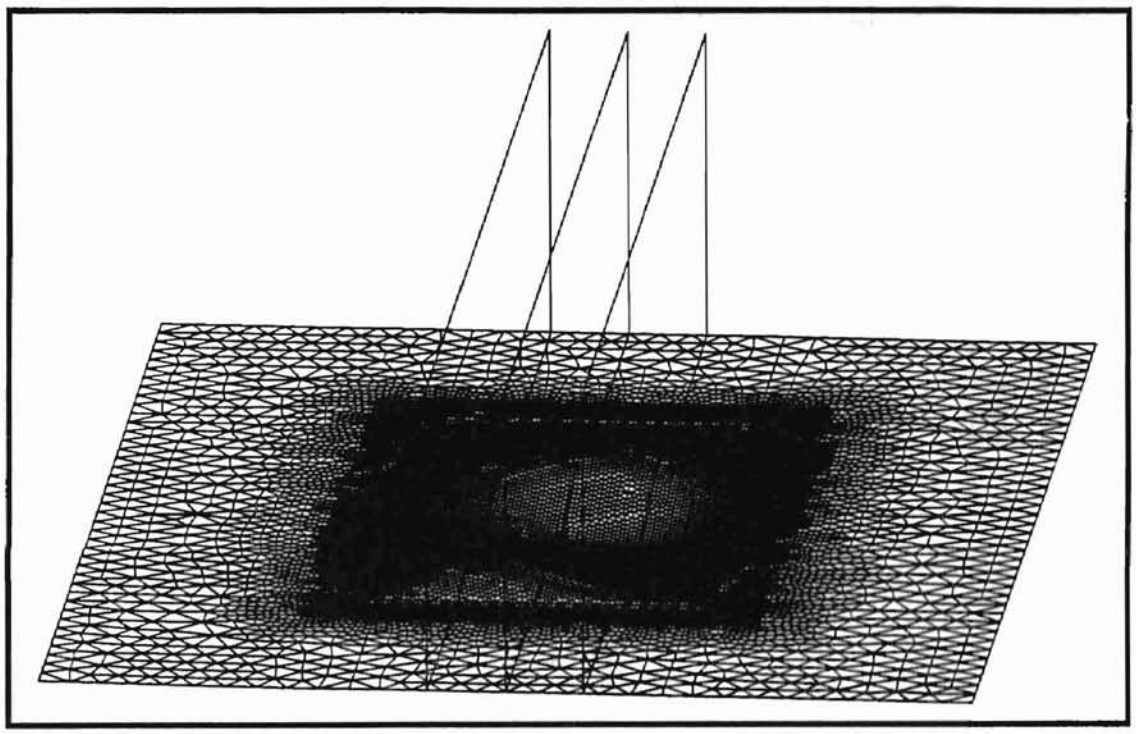

Figure 3.9. Pressure Cut Stations

The pressure profiles at these stations are presented in Figure 3.10.

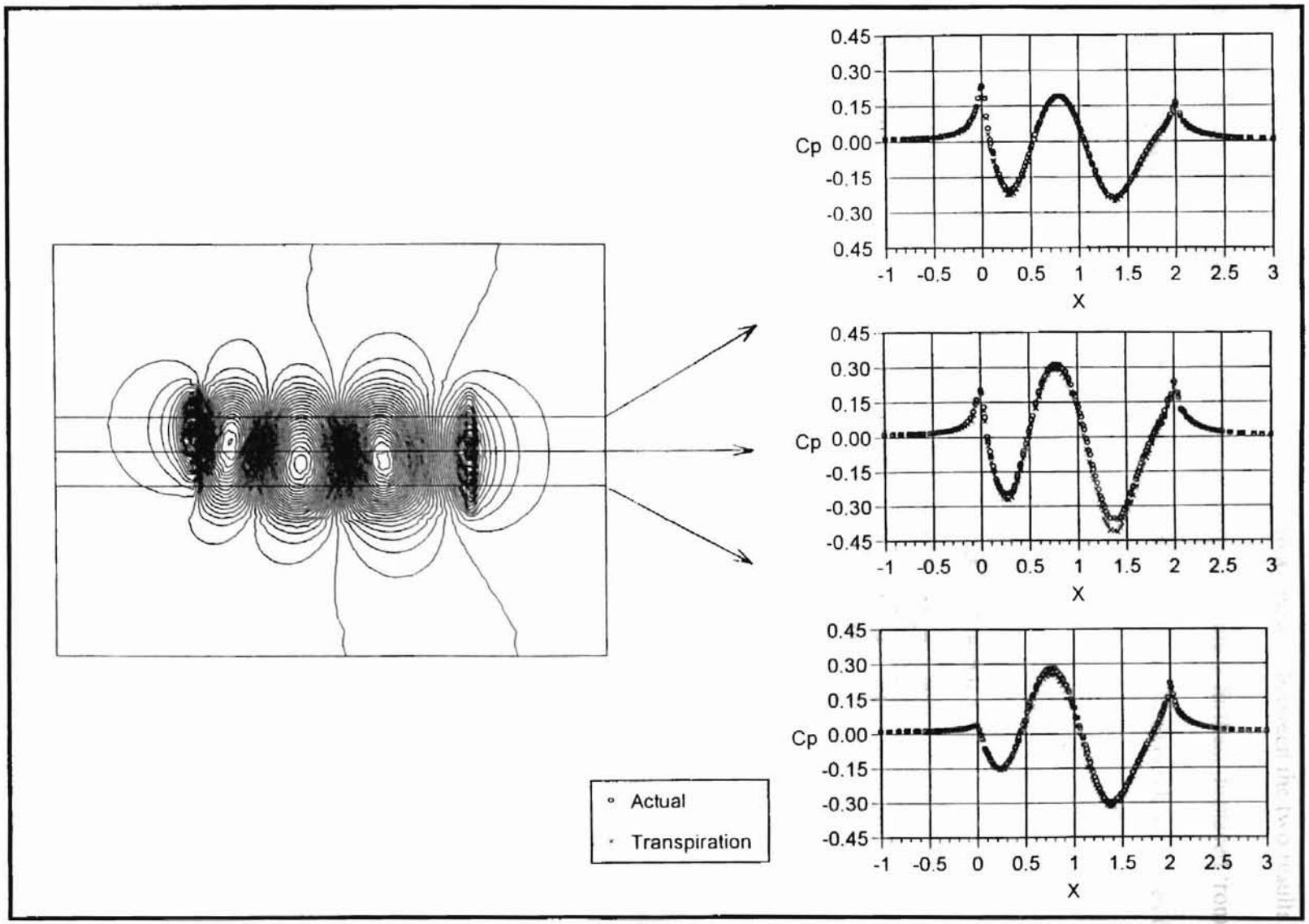

Figure 3.10. Pressure Profiles, Mach 0.3

These pressure profiles show that there is very good agreement between the two results. The largest differences appear to be in regions where the plate is furthest displaced from its original position, which would be expected. Table 3.1 shows the generalized forces for the six modes of each case.

Table 3.1. Generalized Forces for Mach 0.3

Mode	Actual	Transpiration
1	-22.14	-41.66
2	-87.48	-91.38
3	-54.55	-57.12
4	-4.649	-2.229
5	17.65	18.56
6	-57.16	-58.33

The generalized forces are very comparable except in modes 1 and 4. Large differences in generalized forces will be discussed at the end of this section.

The surface pressure contours for the Mach 0.95 case are shown in Figures 3.11 and 3.12.

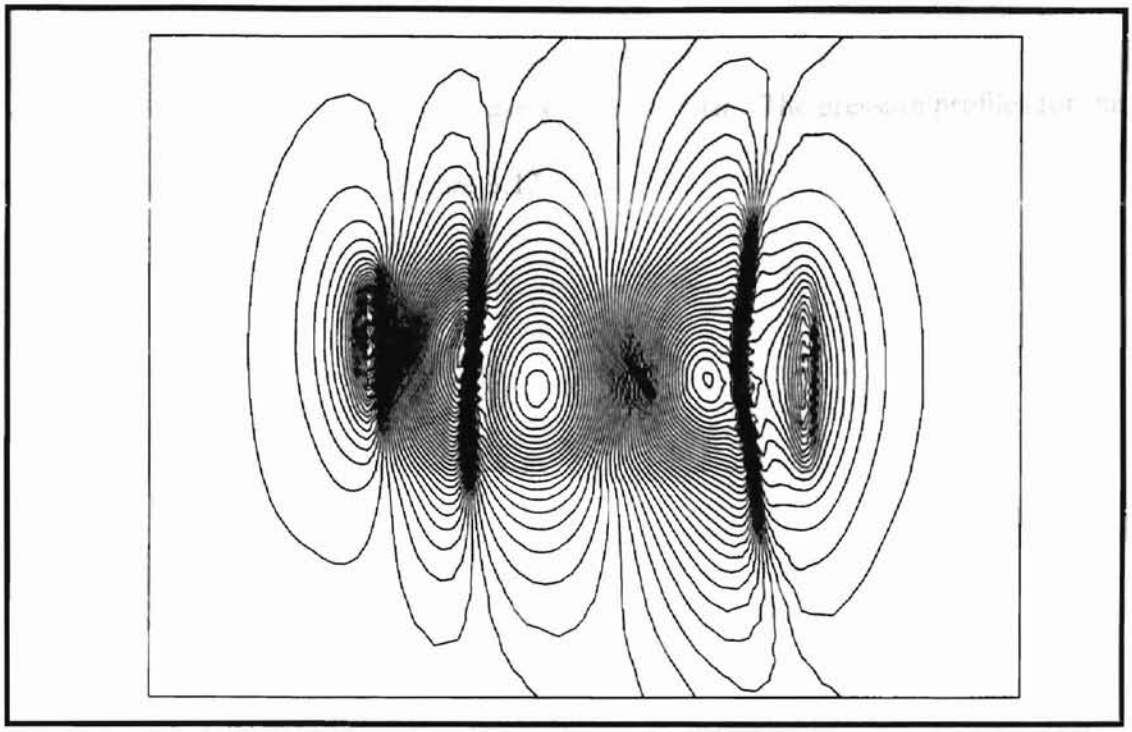

Figure 3.11. Actual Pressure Contours, Mach 0.95

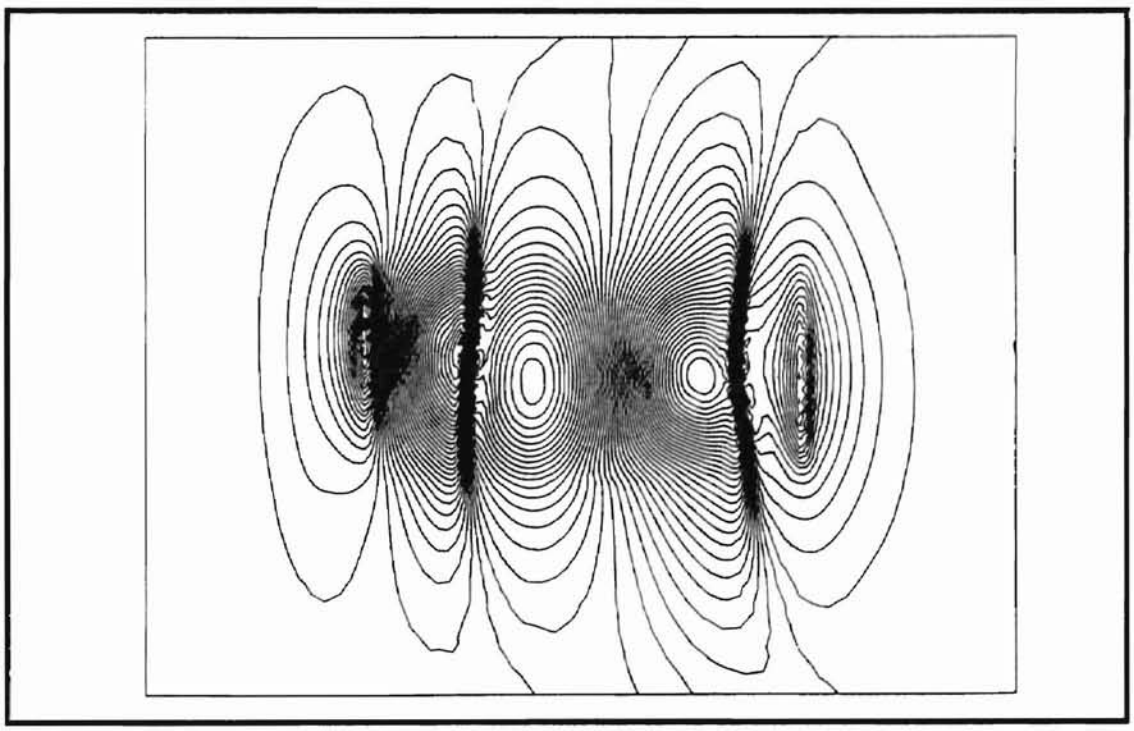

Figure 3.12. Pressure Contours Using Transpiration, Mach 0.95

Again, the pressure contours in each case are very similar. The pressure profiles for this Mach number are presented in Figure 3.13.

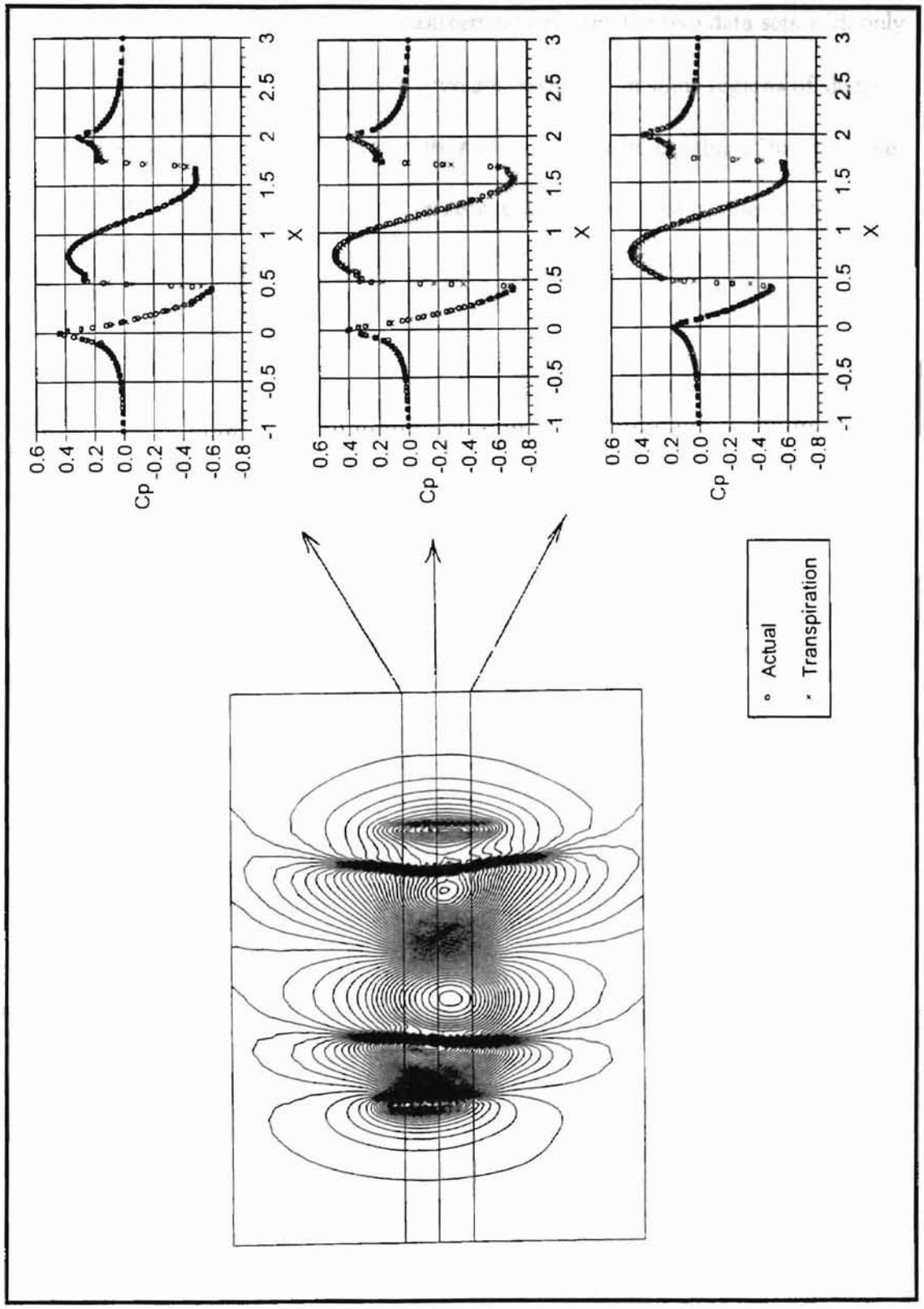

Figure 3.13. Pressure Profiles, Mach 0.95

These pressure profiles show excellent agreement between the two data sets with only slight differences being seen near some pressure peaks and in some regions of sharp pressure changes. The transpiration solution also seems quite capable of handling the formation of the two shocks. This can be seen again in the Mach profiles at the same locations in Figure 3.14.

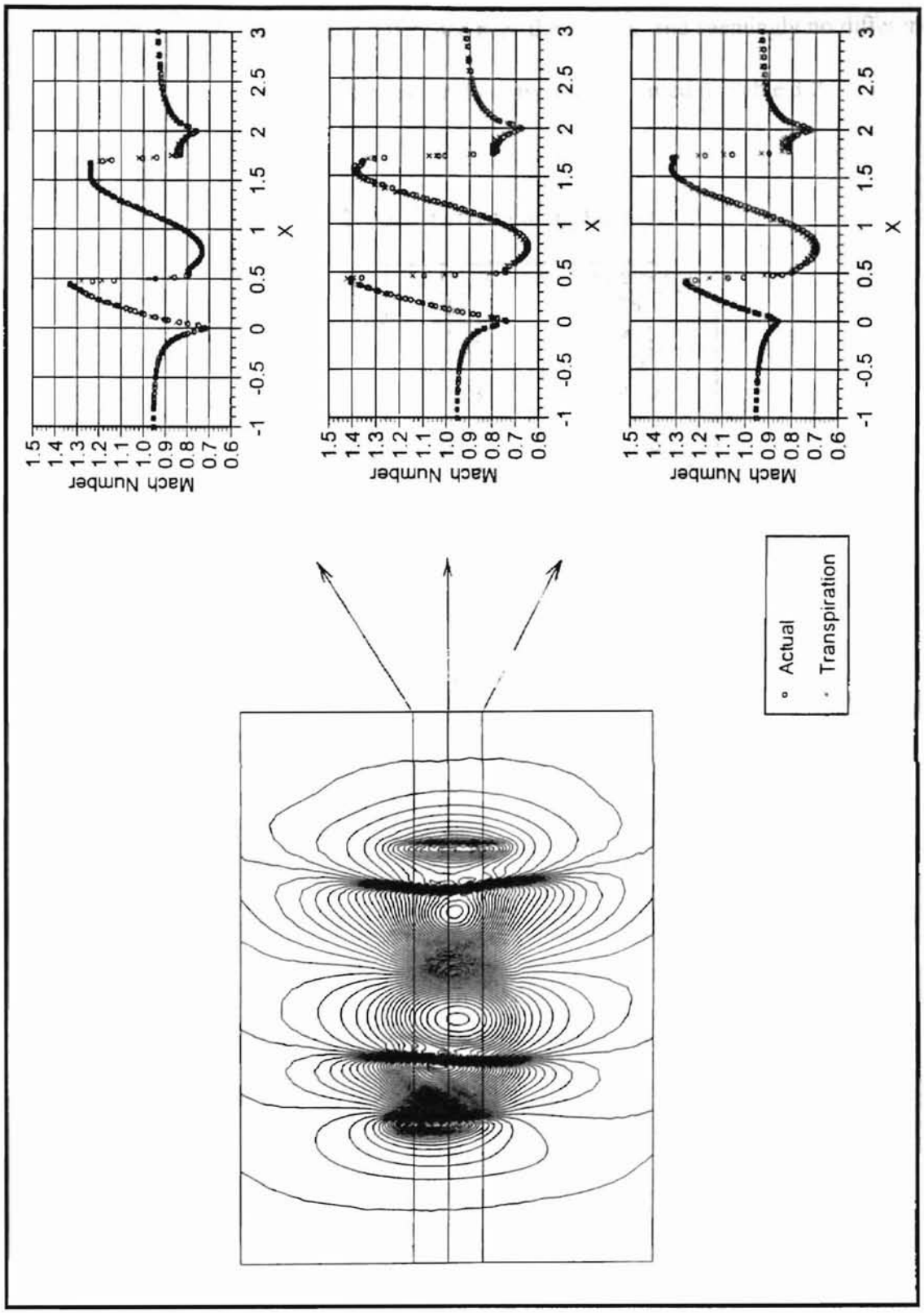

Figure 3.14. Mach Profiles, Mach 0.95

Notice how there are only minor difference near the shocks, and seemingly no differences at the shocks. The generalized forces for this case are presented in Table 3.2.

Table 3.2. Generalized Forces for Mach 0.95

Mode	Actual	Transpiration
1	-283.2	-475.1
2	-1457	-1483
3	-1500	-1495
4	-61.35	-34.72
5	233.5	236.3
6	-869.1	-886.9

These forces are also comparable, with some noticeable differences again being seen in modes 1 and 4.

Figures 3.15 and 3.16 show the surface pressure contours for the Mach 3.0 case.

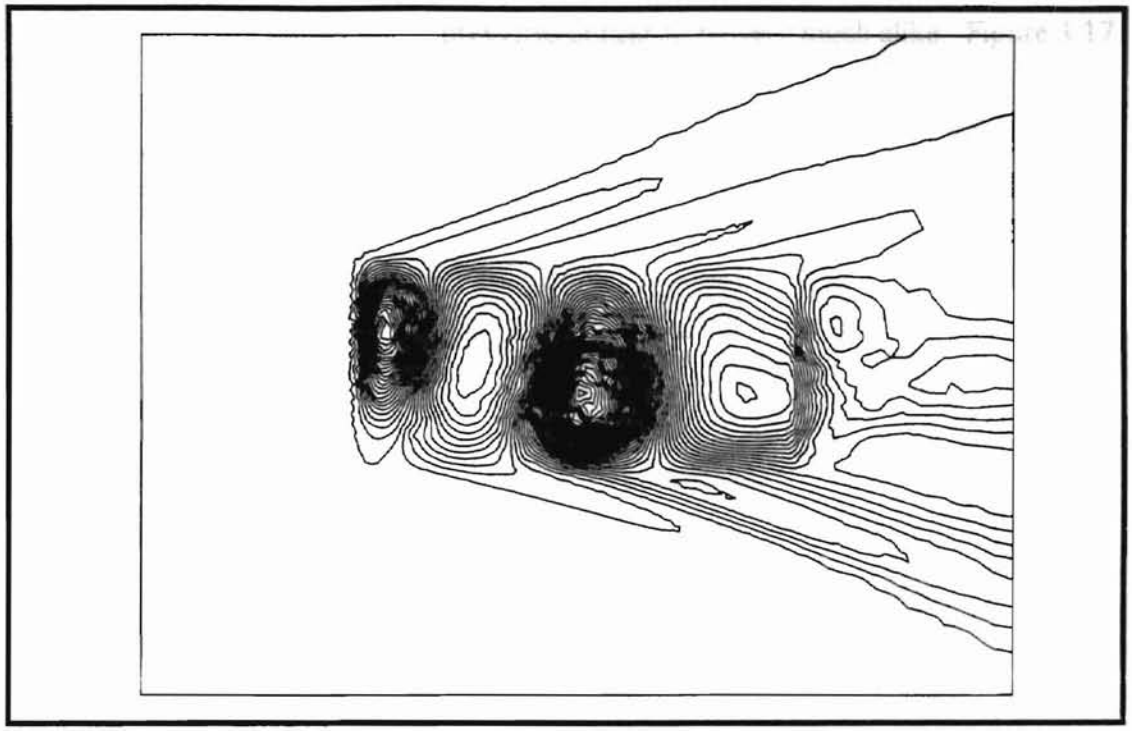

Figure 3.15. Actual Pressure Contours, Mach 3.0

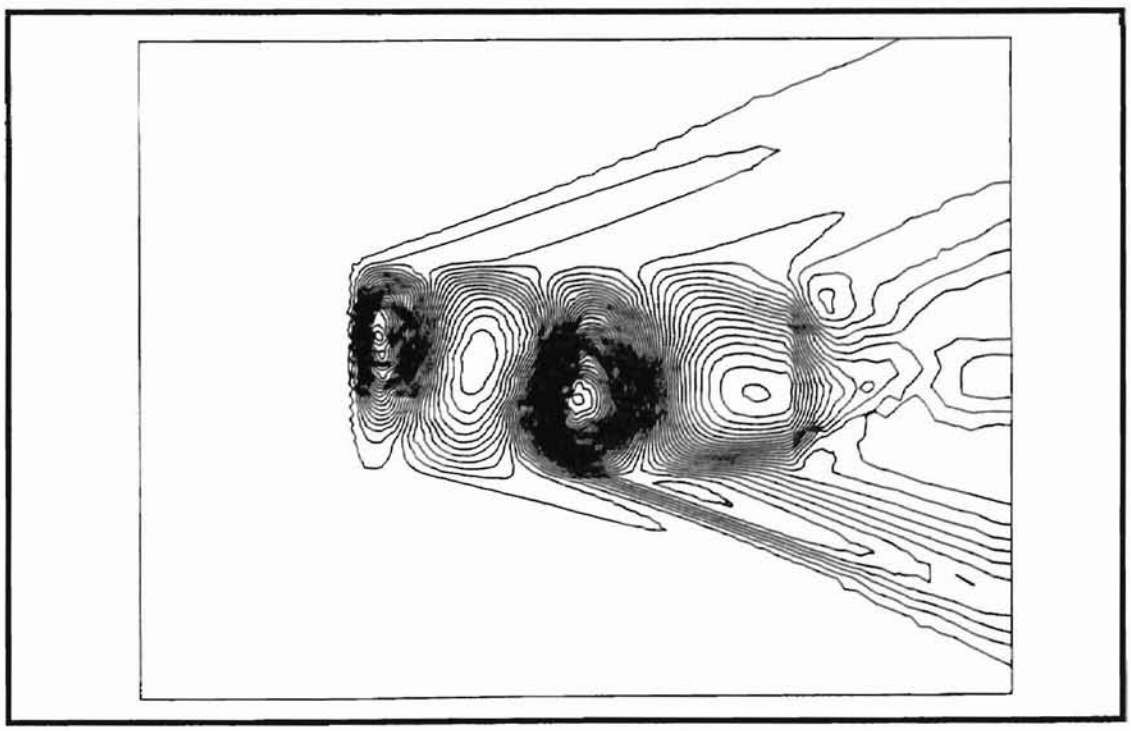

Figure 3.16. Pressure Contours Using Transpiration, Mach 3.0

As in the two previous cases, the pressures appear to be very much alike. Figure 3.17 shows the pressure profiles.

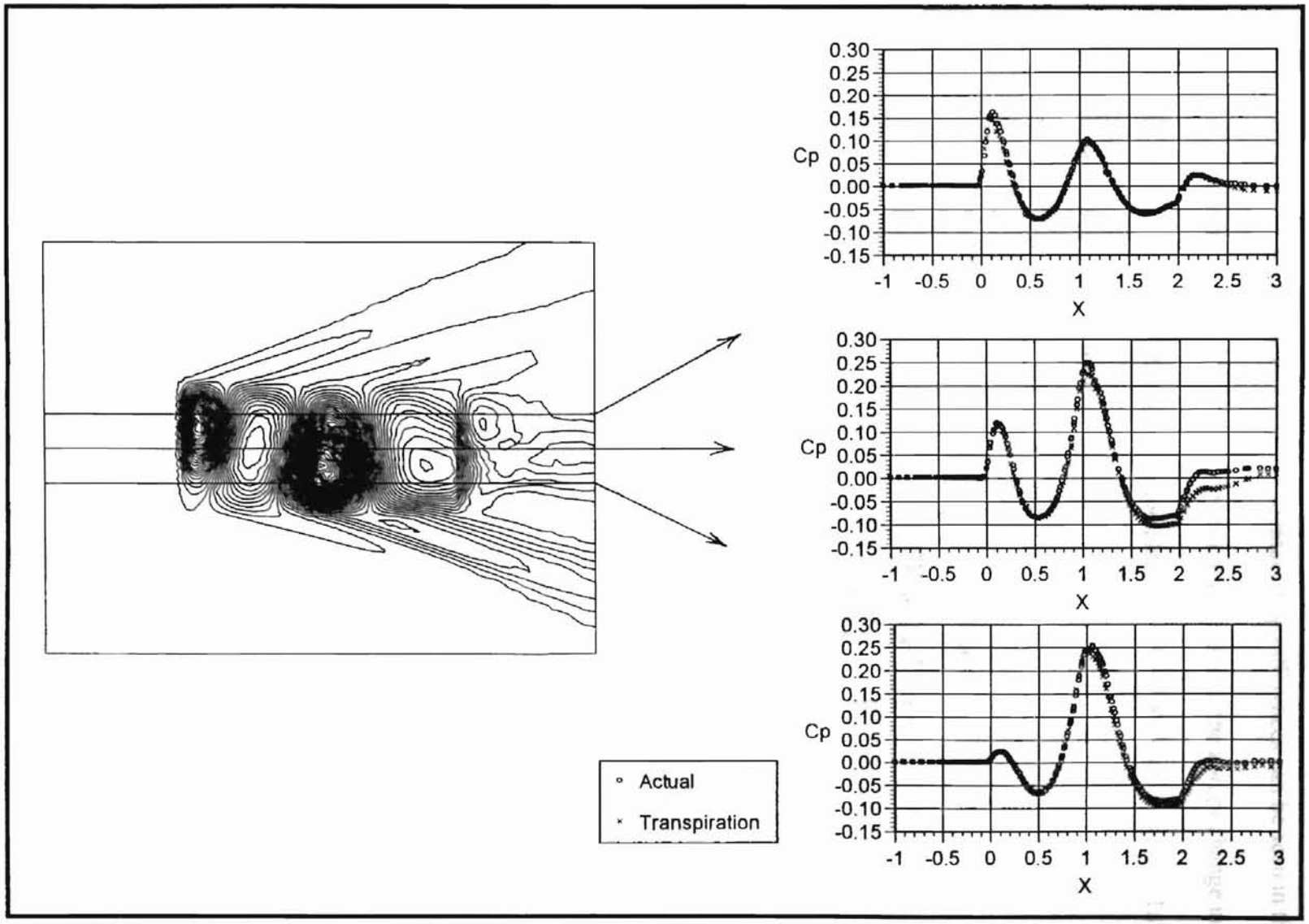

Figure 3.17. Pressure Profiles, Mach 3.0

Most regions show good results, however, some interesting differences can be seen in the region near the end of the plate. These differences could be due to the abrupt change in slope where the plate ends, since the edges of the plate are pinned and not clamped. Table 3.3 gives the generalized forces for this case.

Table 3.3. Generalized Forces for Mach 3.0

Mode	Actual	Transpiration
1	2593	2041
2	534.7	253.1
3	-3708	-3826
4	-848.3	-809.4
5	-574.8	-373.4
6	2248	2194

Here, the differences in generalized forces are seen in modes 2 and 5.

As an illustration of one of the criterion for convergence, the residuals for this case are presented in Figure 3.18.

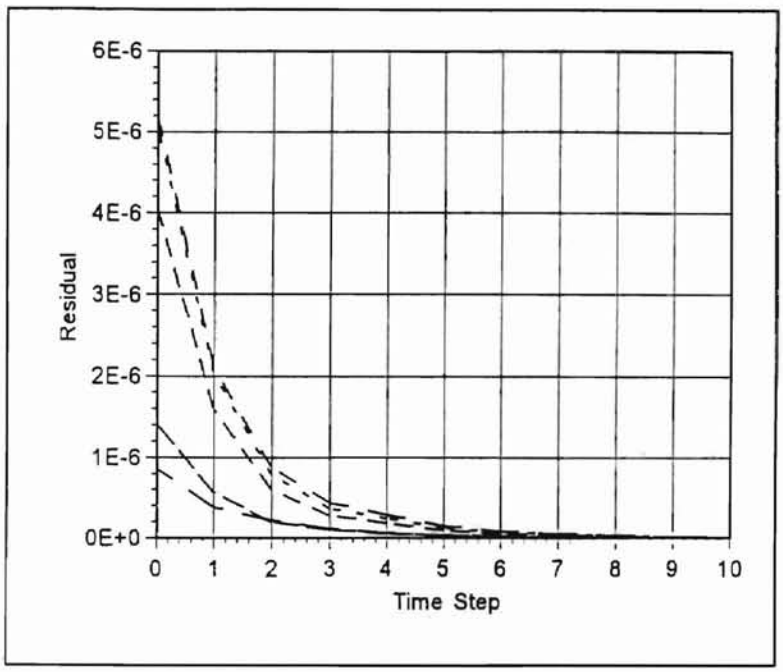

Figure 3.18. Residual Convergence

This shows a well converged solution with final residual values being on the order of 10^{-10}.

It is evident from these plots that transpiration very accurately simulates the deflection. However, this is not readily assumed when studying the generalized forces. Since the surface pressures match so closely, it can be deduced that generalized forces may be very sensitive to small differences in surface pressures. However, differences may be negligible if the structural spring force is large relative to the generalized forces. Also, since in one case there is actual plate deformation while in the other case the deflection is only simulated, the internal mesh of each domain will be different. Subsequently, as will be shown in later sections, the solution can be strongly dependent on the mesh. Therefore,

not all of the differences seen can necessarily be attributed to the transpiration boundary condition.

3.4. AGARD 445.6 Wing

The next case that was investigated was the AGARD 445.6 wing. This wing is a standard aeroelastic test configuration which has been investigated experimentally in the Langley Transonic Dynamics tunnel. Using this wing allows for transpiration comparison in practical application. Also, in this case, the surface is surrounded by the flow unlike the plate case where the flow is only on one side, thus adding to the complexity of the problem. The original, undeflected wing is shown in Figure 3.19.

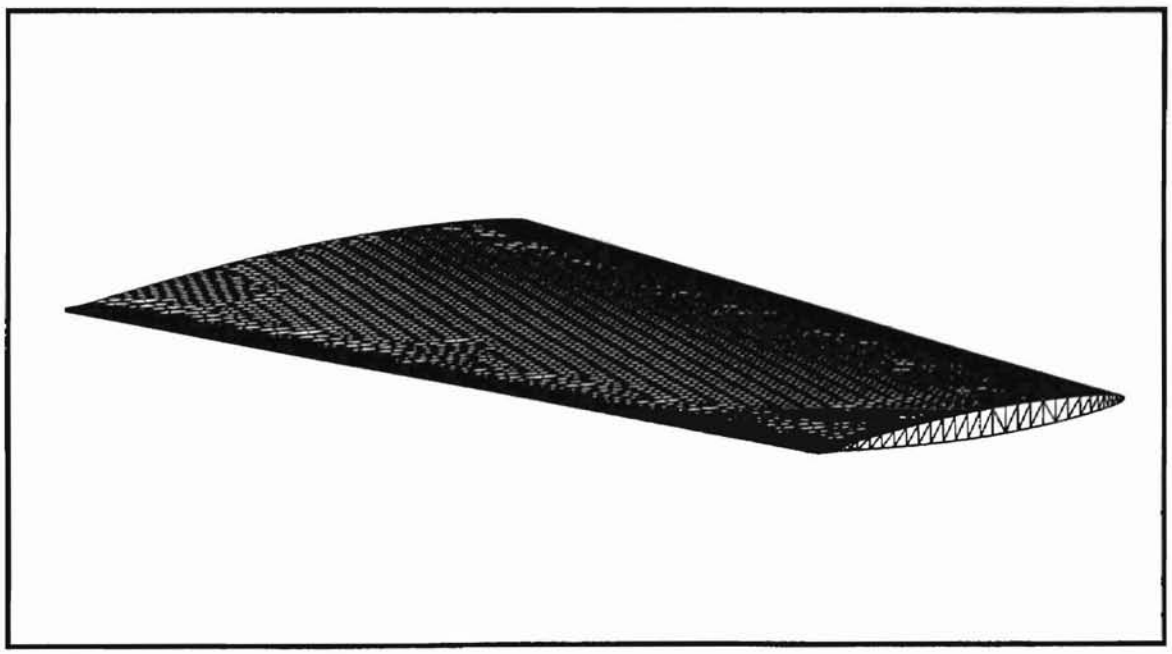

Figure 3.19. AGARD Wing

The wing was given a generalized displacement of 2 units in first mode bending and 2 units in first mode torsion. The deflected wing is shown in Figure 3.20.

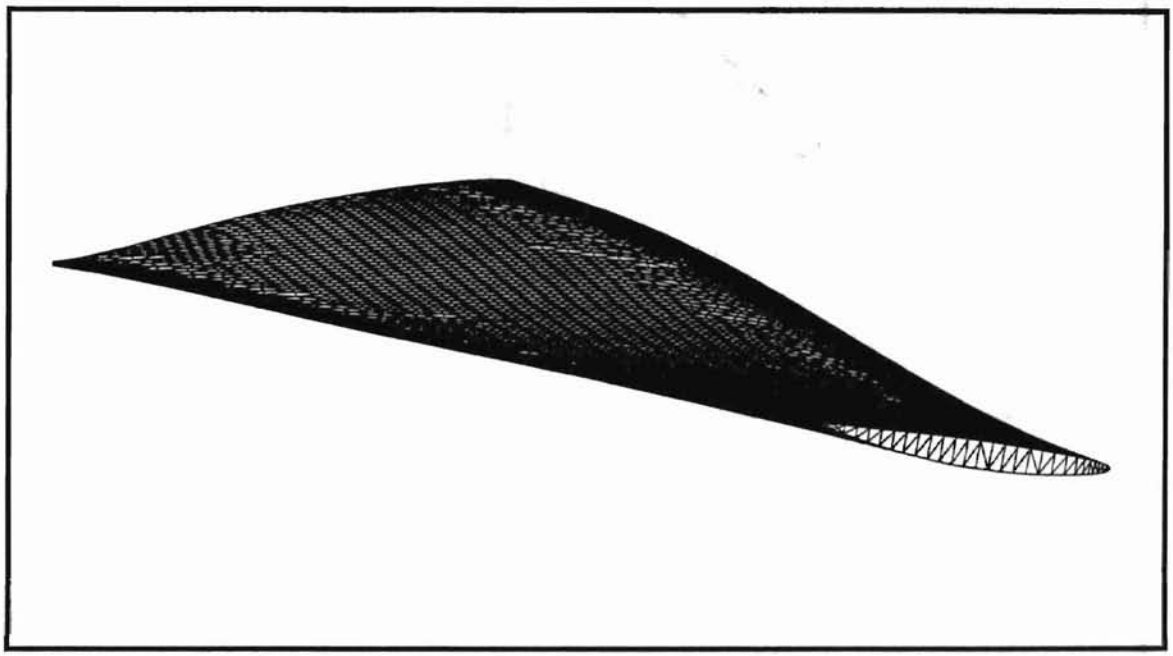

Figure 3.20. Deflected AGARD Wing

The severity of the deflection is apparent from this figure. It is so significant that an approximate -9 degree angle of attack is created at the tip of the wing where there should be none. In addition, the end of the wing has translated below its original position. Results were obtained for Mach numbers of 0.99, 1.141, and 2.0, using this deflection. Even with this unrealistic deformation at these Mach numbers, transpiration produces a very accurate simulation.

The surface pressure contours on the lower surface of the wing for Mach 0.99 are shown in Figures 3.21 and 3.22.

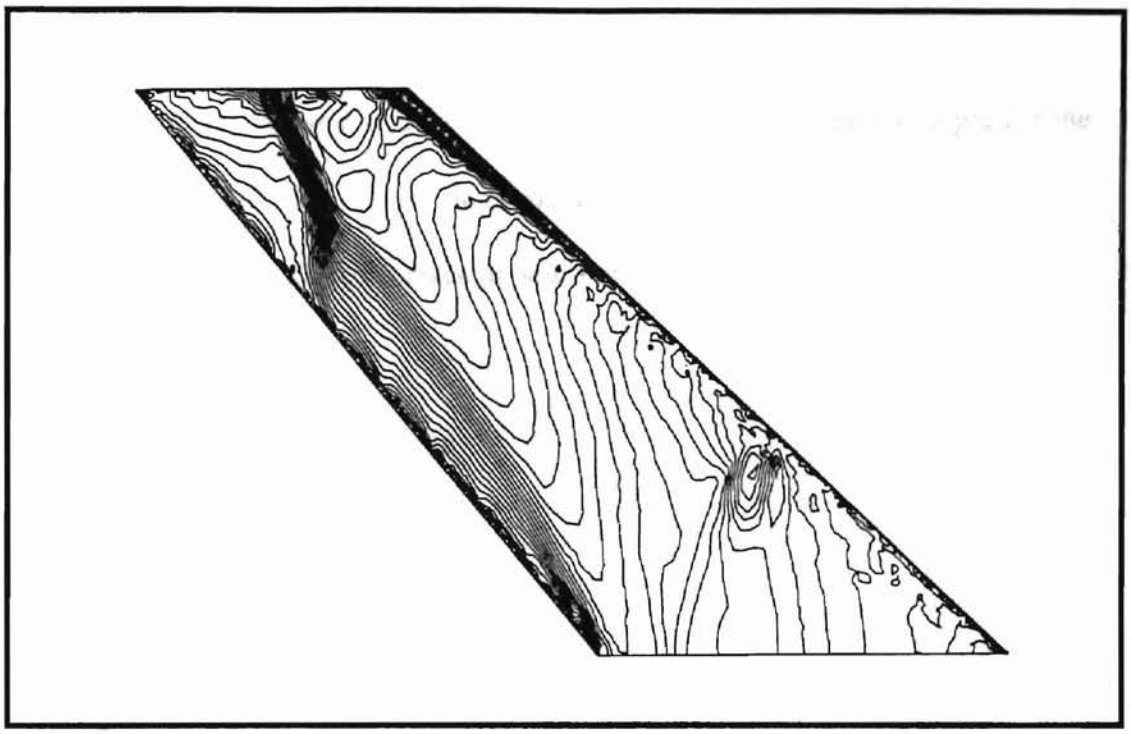

Figure 3.21. Actual Pressure Contours, Mach 0.99

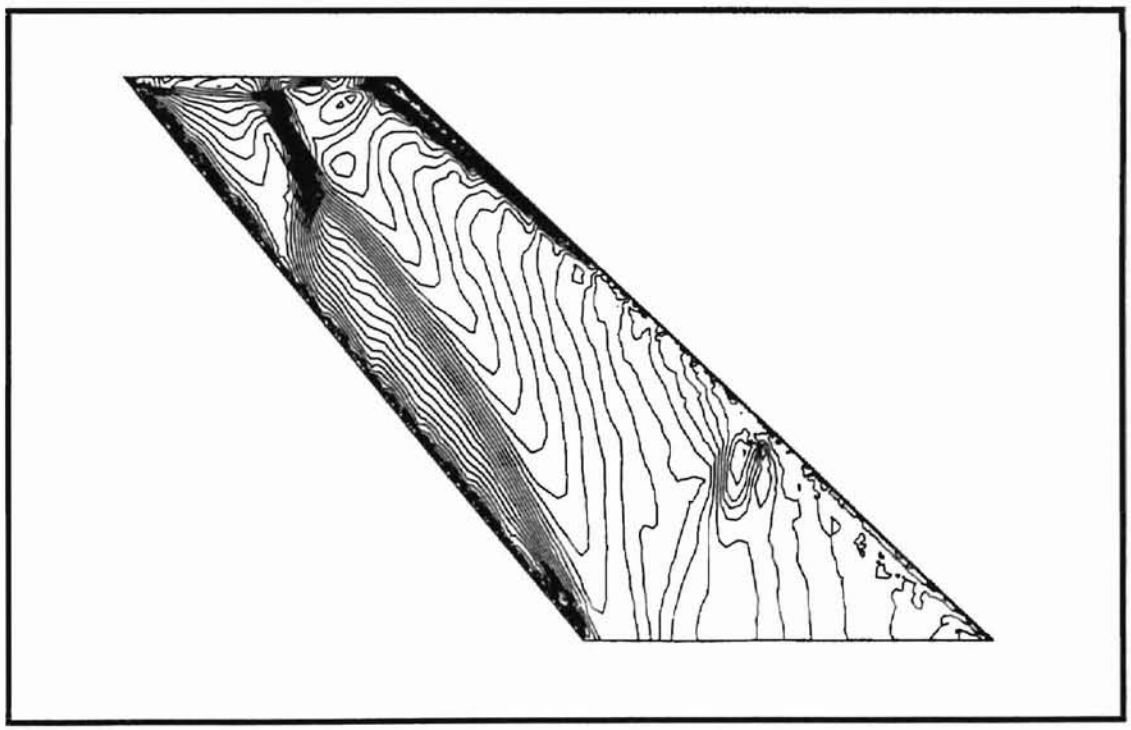

Figure 3.22. Pressure Contours Using Transpiration, Mach 0.99

Both results show the same regions of strong pressure gradients and both predict the formation of a shock near the middle of the tip of the wing.

Actual and simulated surface pressure profiles at three stations for the Mach 0.99 are shown in Figure 3.23.

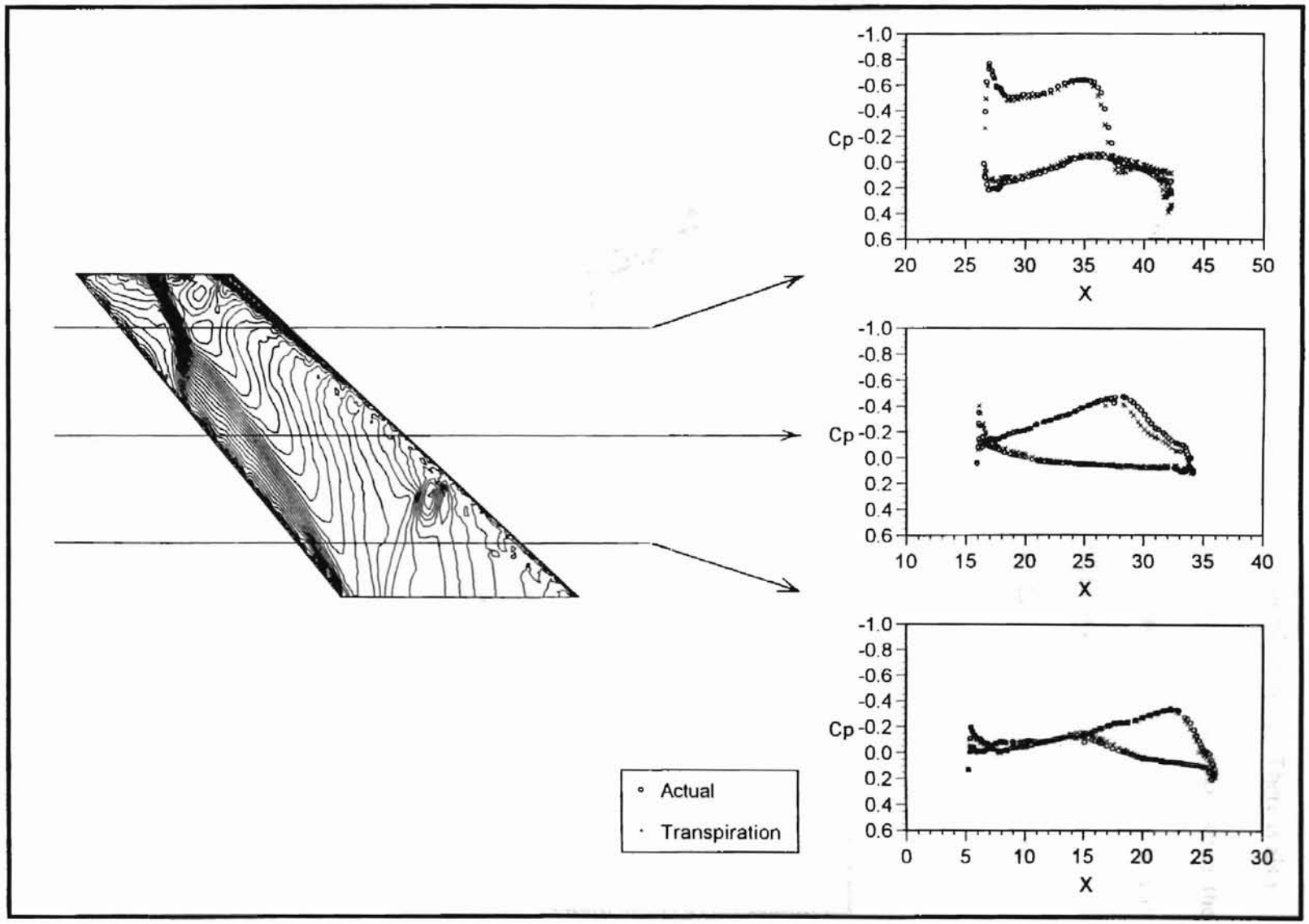

Figure 3.23. Pressure Profiles, Mach 0.99

The two data sets show very good agreement near the root of the wing. There is also good agreement near the tip of the wing except very close to the trailing edge, where the transpiration solution predicts a larger pressure peak. The largest differences are seen at the middle of the wing where the data is somewhat shifted near the trailing edge.

Surface pressure contours are presented for the Mach 1.141 case in Figures 3.24 and 3.25, again for the lower surface.

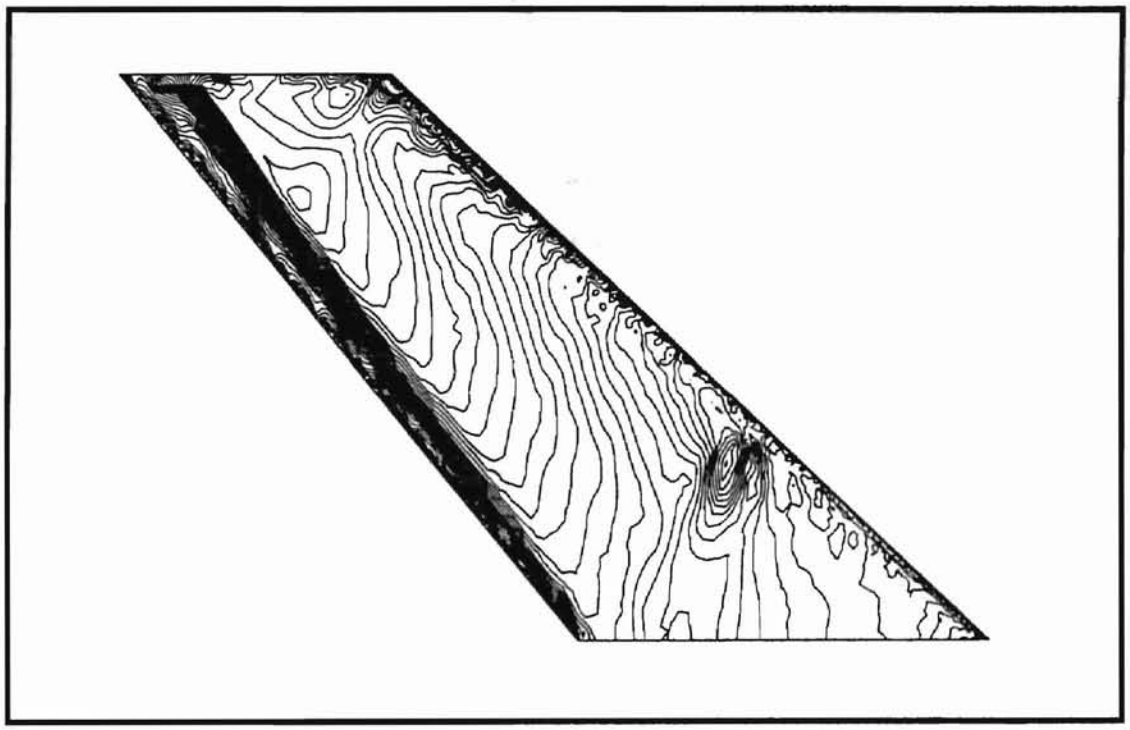

Figure 3.24. Actual Pressure Contours, Mach 1.141

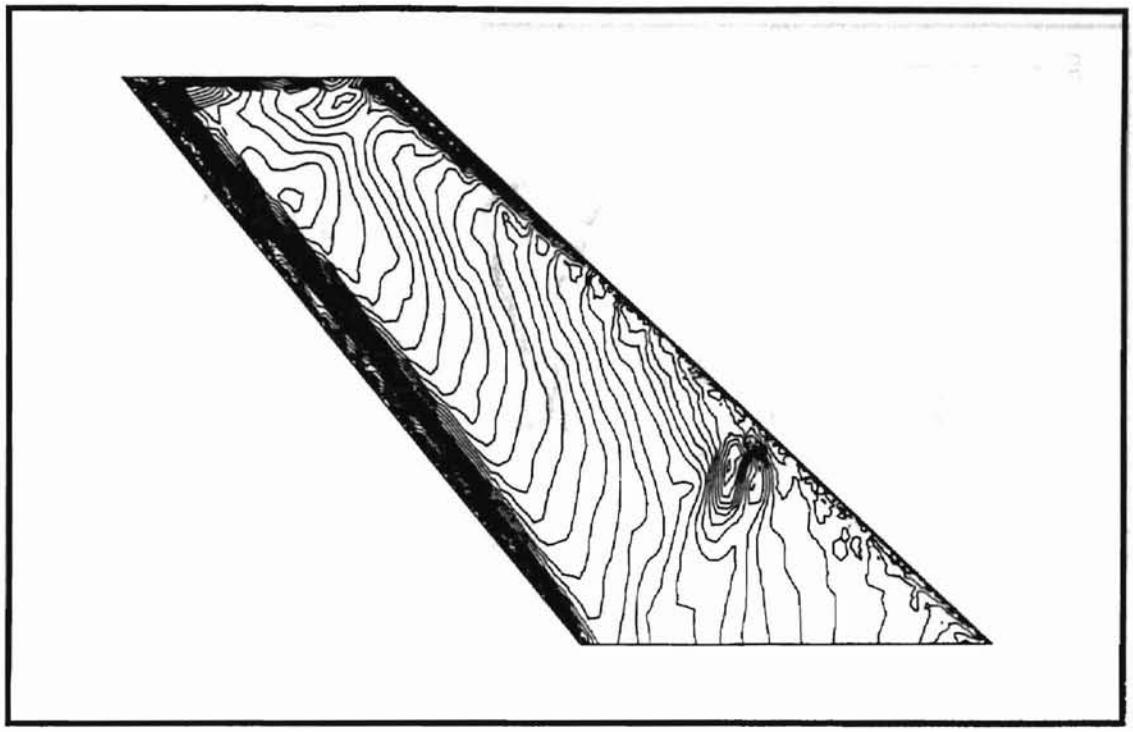

Figure 3.25. Pressure Contours Using Transpiration, Mach 1.141

Overall, the results appear to be very good from studying the pressure contours. The pressure profiles for this case are presented in Figure 3.26.

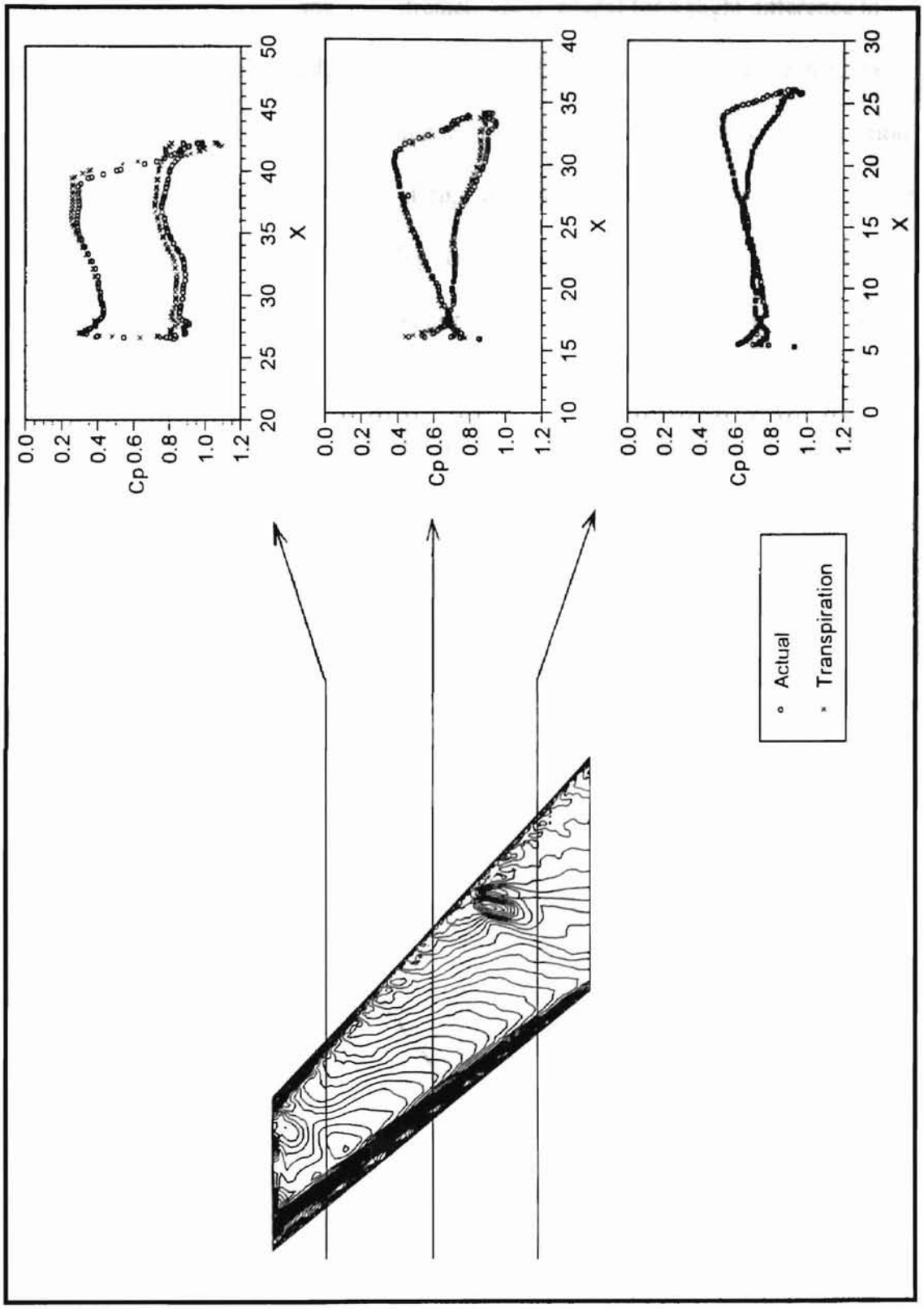

Figure 3.26. Pressure Profiles, Mach 1.141

Results near the root of the wing are extremely good, except for a slight difference in pressure peaks at the trailing edge. The agreement decreases with increasing distance from the root. This demonstrates the limitation described in Section 3.1 of transpiration not accounting for actual surface translation, since the wing is increasingly displaced from its unmodified position moving from wing root to tip. However, despite the very large deflection and rotation at the tip, the results there are quite good, with the largest percent error being less than 15%.

The surface pressure contours on the lower surface for the Mach 2.0 case are shown in Figures 3.27 and 3.28.

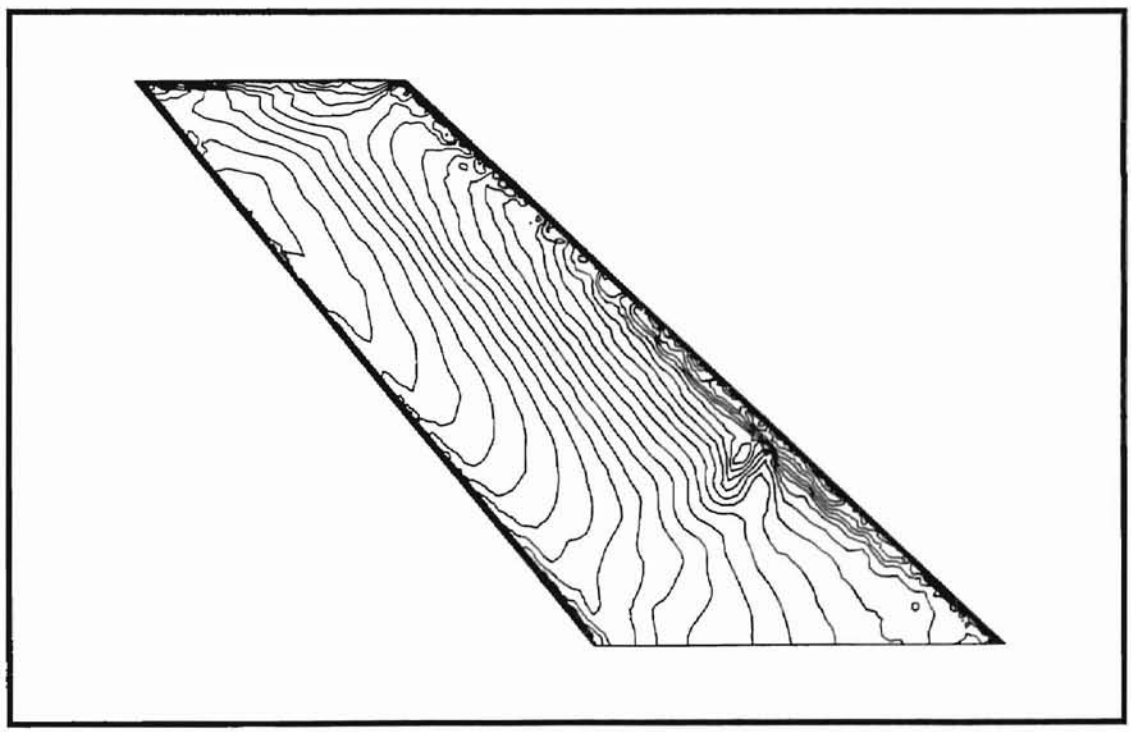

Figure 3.27. Actual Pressure Contours, Mach 2.0

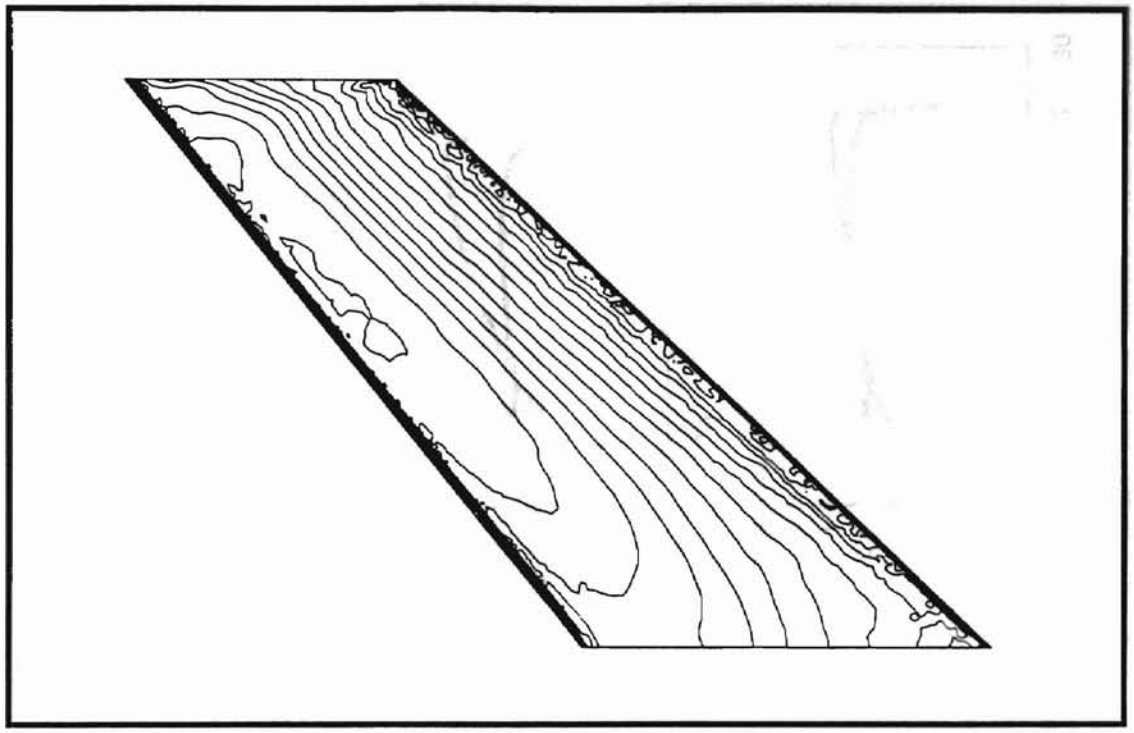

Figure 3.28. Pressure Contours Using Transpiration, Mach 2.0

Strong pressure gradients can be seen near the leading and trailing edges in both cases. The pressure change from leading edge to trailing edge appears to be more uniform in the transpiration case than in the actual deflection. However, in both cases the pressure gradient in this region is small, therefore small differences are somewhat magnified. The small differences are more evident in the surface pressure profiles shown in Figure 3.29.

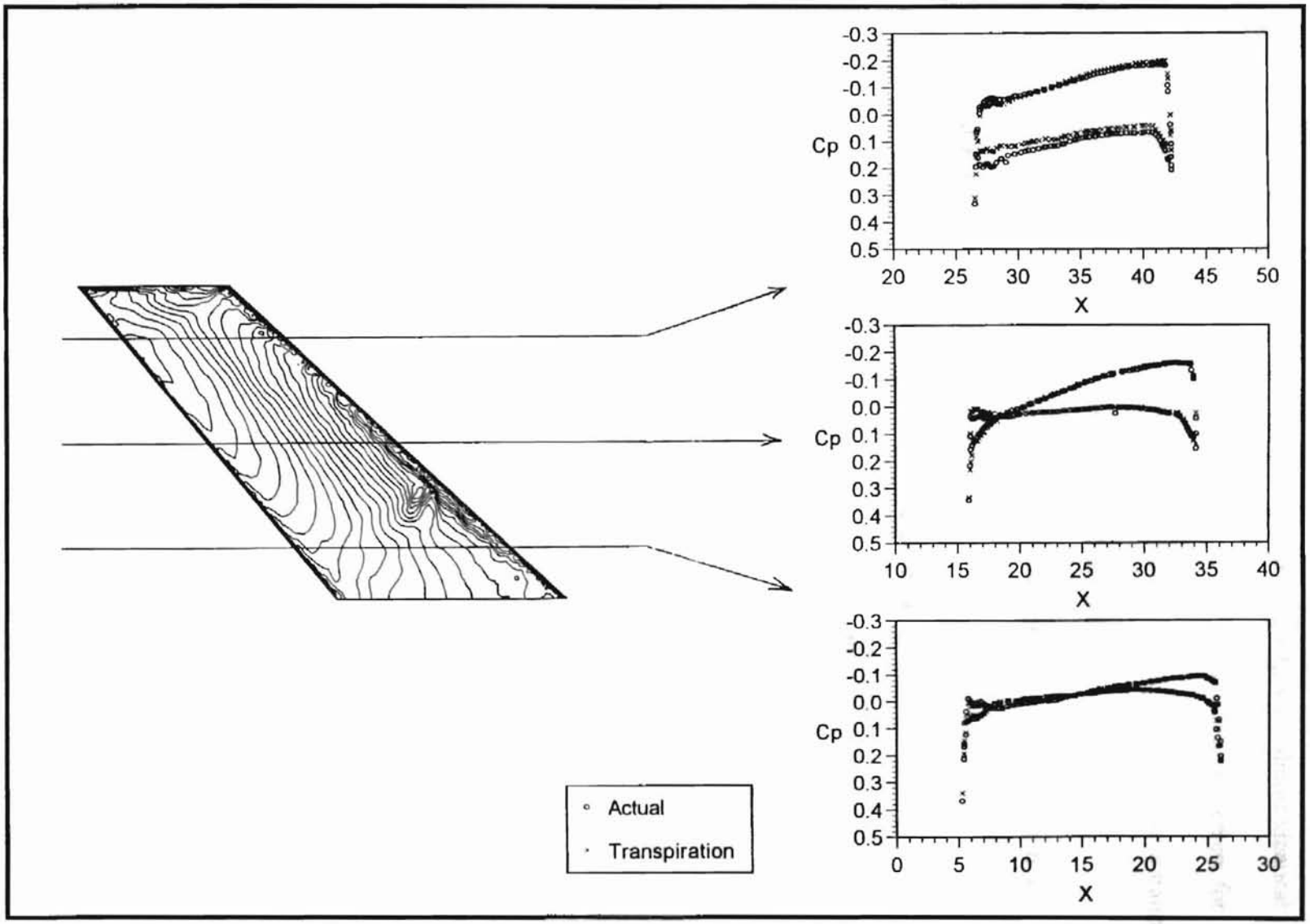

Figure 3.29. Pressure Profiles, Mach 2.0

Notice that the pressures away from the leading and trailing edges are almost identical near the root and middle of the wing. In fact, there is very good overall agreement for these two stations, with slight differences seen near the leading edge at the middle station. Again, the station near the tip shows the largest differences, as expected.

This wing was also studied with generalized displacements of 2.63 units in first mode bending and 0.33 units in first mode torsion. Comparisons were made for Mach numbers of 0.678, 0.99, and 2.0. These results are presented in the Appendix.

All of these cases clearly show that transpiration is effective at simulating even relatively large deflections in transonic and supersonic flows. Another point in the application of transpiration is in flutter studies of a severly deflected body, such as this one. Rather than using methods such as deforming meshes or transpiration to deflect the surface and perform flutter investigations, it would be simpler and possibly more accurate to perform the steady solution on the actually deflected surface, then perform the unsteady aeroelastic analysis from this solution. The deflected surface could be obtained using methods in this study, and the flutter solution could be determined with confidence using transpiration, since it is known to be accurate in simulating small disturbances.

As previously mentioned, some discussion of the sensitivity of the mesh to the flow solution is necessary so that all solution differences will not be falsely attributed to transpiration. This discussion is presented in the following section.

3.5. Mesh Sensitivity

The original plate mesh was much less refined than the one that was used to obtain the results presented in plate section. The original mesh is shown in Figure 3.30.

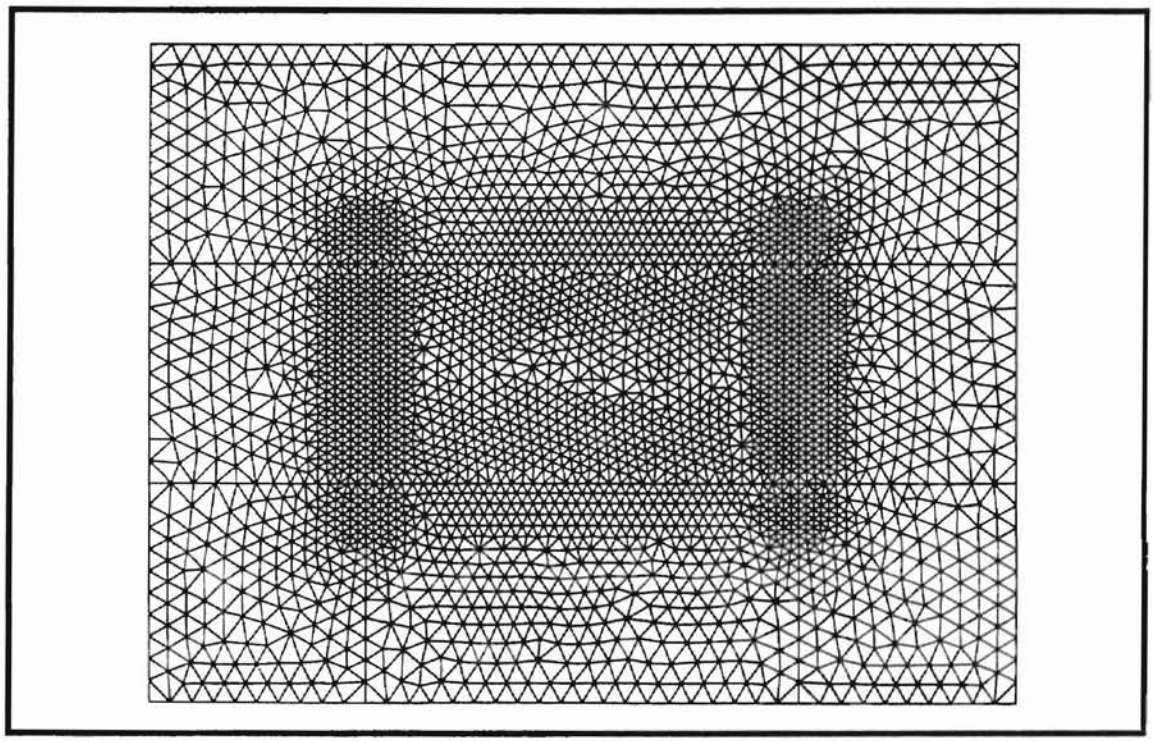

Figure 3.30. Original Plate Mesh

When observing the solutions from this original mesh, it was apparent that the elements were too small and too few to make the solution smooth. Therefore, the solution was probably somewhat inaccurate. A new mesh was constructed to produce a more accurate solution. This mesh was presented in Figure 3.4.

Pressure profiles are presented in Figure 3.31 for both the new and old actually deflected meshes for 0.1 generalized displacements at Mach 3.0.

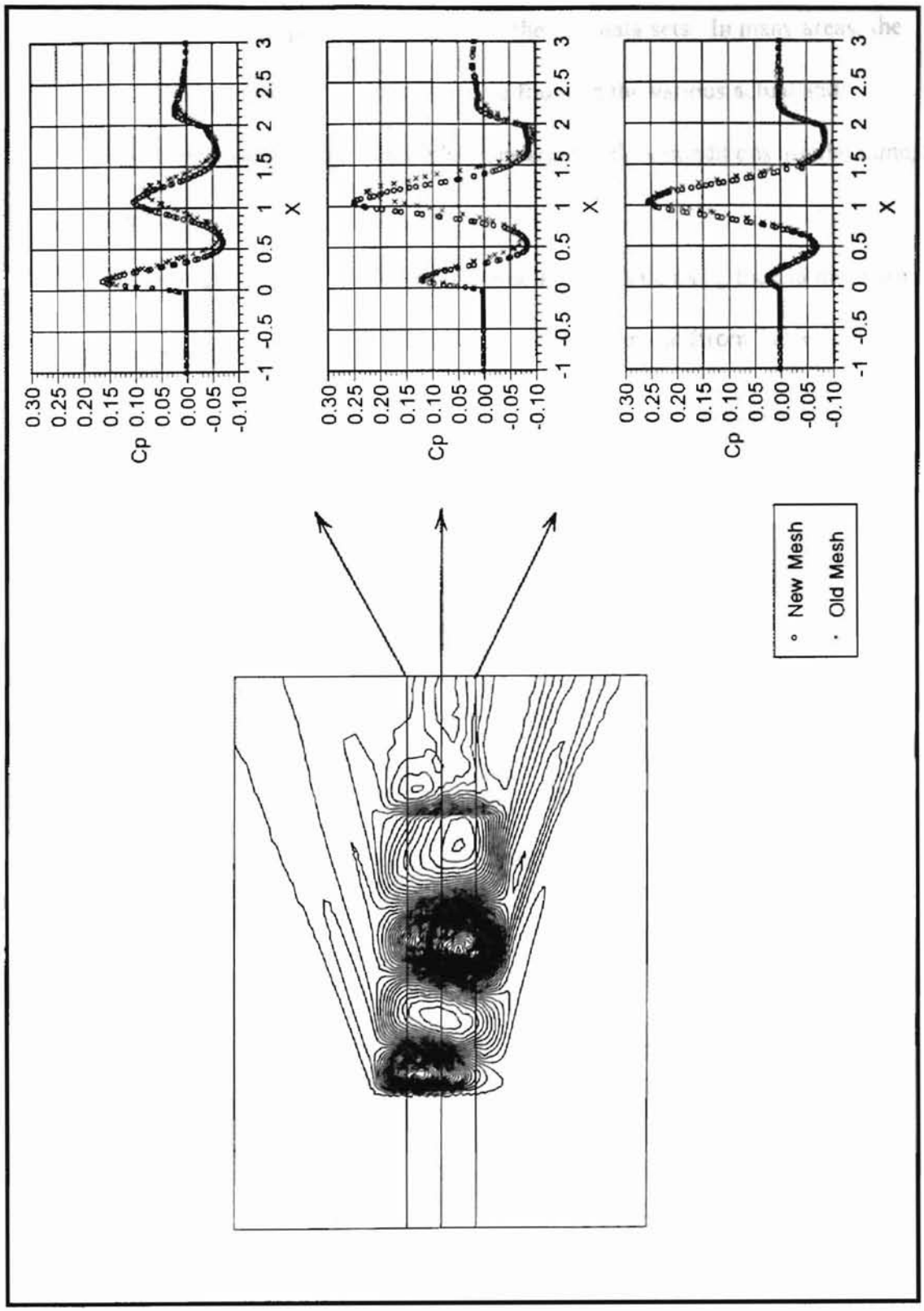

Figure 3.31. Pressure Profiles for New and Old Plate Cases

Some rather large differences are seen between the two data sets. In many areas, the differences are larger than differences that were found in the various actual and transpiration comparisons. Since the deflections and the flow conditions are the same, the difference must be the mesh.

The generalized forces that were obtained for the plate using the old mesh are presented in Table 3.4 along with the values from the new mesh (from Table 3.3).

Table 3.4. Generalized Forces for Old and New Meshes

Mode	Old Mesh	New Mesh
1	2718	2593
2	1274	534.7
3	-2564	-3708
4	-842	-848.3
5	-2872	-574.8
6	713	2248

There are significant differences in the two sets of values. Again, in some cases, the differences are larger than differences between actual and transpiration results.

Obviously, the more refined the mesh, the more accurate the solution will be. However, a more refined mesh contains more elements and nodal points, thus requiring more computational effort. The investigator must determine a balance between accuracy and practicality. Due to this mesh sensitivity, a final case was investigated where only one mesh was used to obtain comparison results. This case is presented in the following section.

3.6. Plate with 0.5 Generalized Displacements

Since transpiration produced good results in the first plate case presented, a plate deflection 5 times greater than that of the first was used. As mentioned, the flow solution can be dependent on the mesh. Therefore, to eliminate error introduced by mesh differences, actual deflection results were not compared to transpiration results. Instead, transpiration was used with the deflected plate to simulate a flat plate. Ideally, the solution to a problem of this type should be equivalent to the flow across a flat plate, where the surface pressures and the generalized forces are zero, and the Mach number is equal to the freestream everywhere.

The superposition of modes for this case is shown in Figure 3.32.

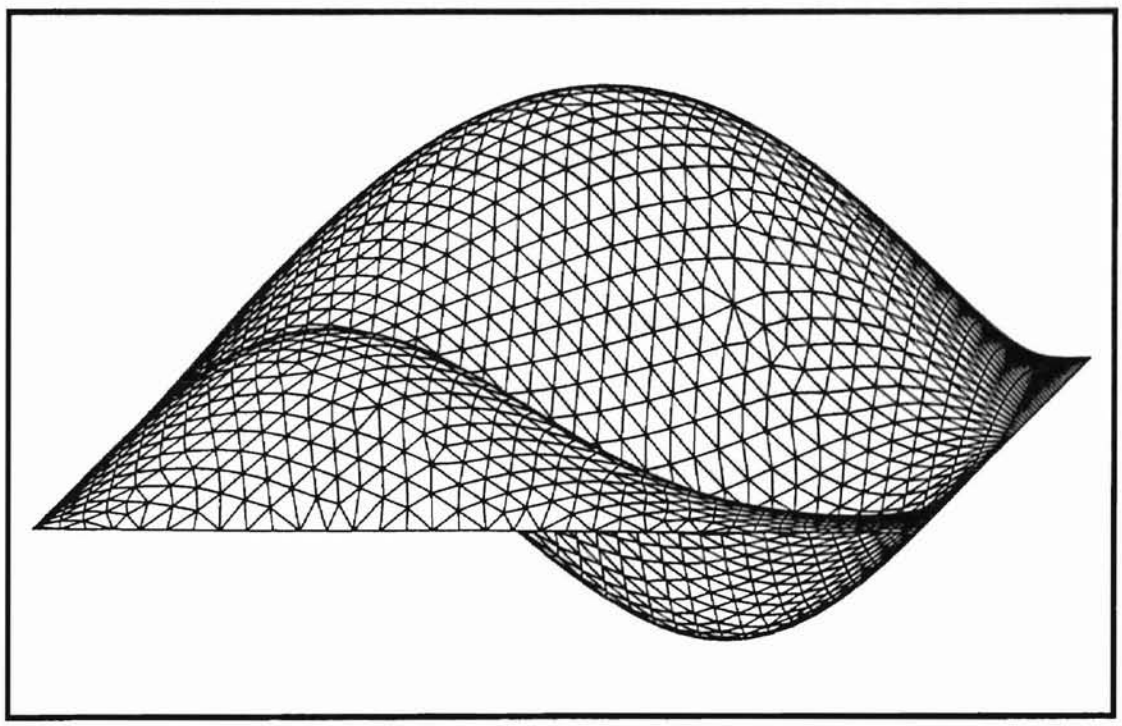

Figure 3.32. Deflected Plate, 0.5 Generalized Displacements

The remarkable amount of deflection is obvious from the figure. The deflection is so significant that it produces maximum displacement that is greater than 35% of the width. Solutions were obtained for Mach numbers 0.3, 0.8, 0.95, and 3. In each case, a well converged deflected solution was used as the starting point for the transpiration solution. In all cases, transpiration was effective in "removing" the deflection. However, results for the Mach 0.95 case were not as good as the others after the same number of iterations.

A summary of the final results for this case is given in Table 3.5.

Table 3.5. Summary of Results for 0.5 Generalized Displacement Plate

	Mach 0.3	Mach 0.8	Mach 0.95	Mach 3.0
Mach Number	0.3 ± 0.00001	0.8 ± 0.00005	0.95 ± 0.04	3.0 ± 0.001
Pressure Order of Magnitude	10^{-6}	10^{-4}	10^{-3}	10^{-6}
Average Percent Difference in GFs	2.98e-6	1.62e-5	8.27e-3	5.23e-6

From the table it can be seen that the overall Mach number becomes approximately the freestream Mach number in each case. Also, the surface pressures in each case are essentially zero with respect to their original deflected values, which were on the order of 10^{-1} to 10^{0}. The average percent error in generalized forces was calculated by averaging all of the ratios of final force value and initial force value for each mode. As an illustration of the generalized forces approach to zero, a plot of the generalized force time history for Mach 3 is presented in Figure 3.33.

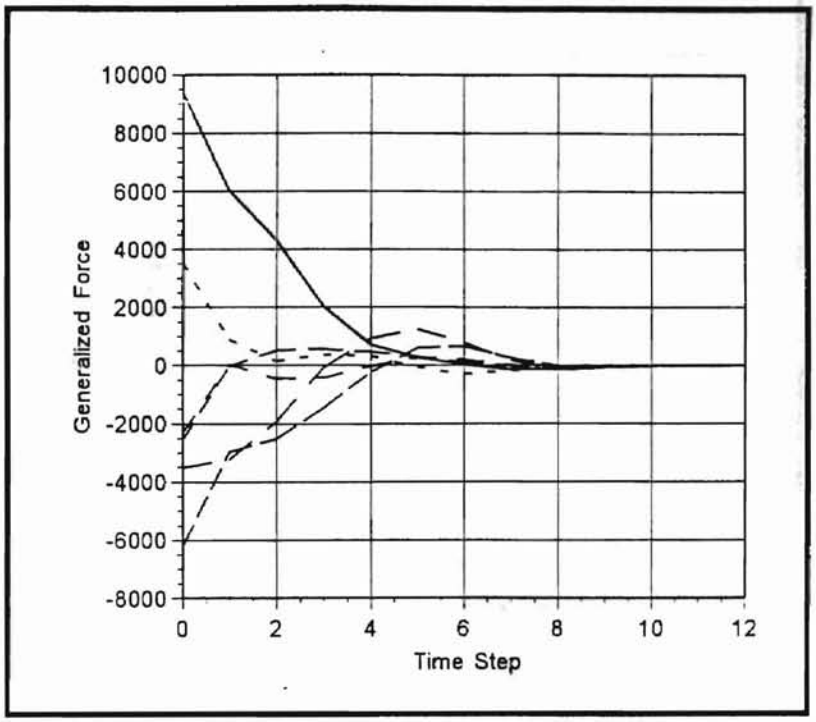

Figure 3.33. Time History of Generalized Forces

This plot is representative of the time history of generalized force for each of the other Mach numbers as well.

A plot of average percent error versus Mach number is presented in Figure 3.34.

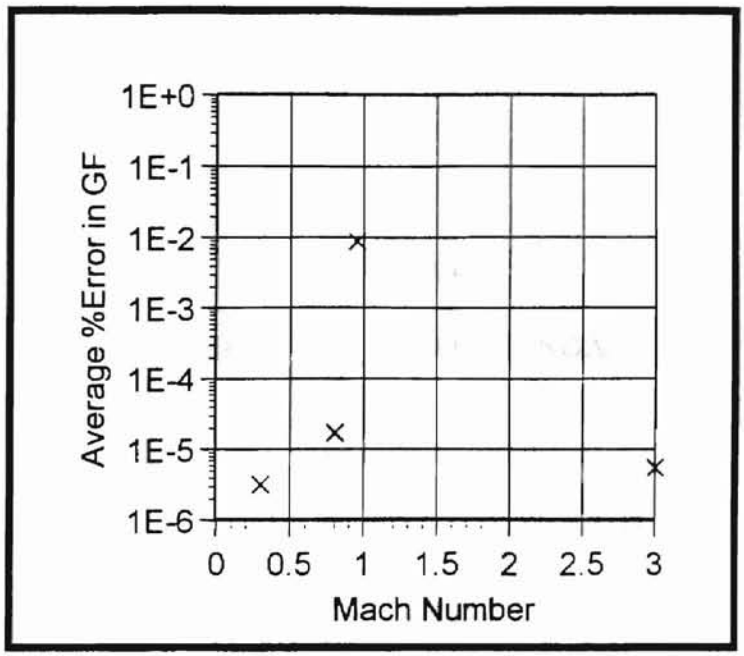

Figure 3.34 Average Percent Error in Generalized Forces

This plot suggests that transpiration was less effective in removing the deflection in the transonic range. However, since transpiration did not appear to be less effective in the other cases in the transonic range, a generalization cannot be made. Overall results for this case are very good, considering the magnitude of the deflection that is being "removed" by transpiration.

CHAPTER 4

CONCLUSIONS AND RECOMMENDATIONS

4.1. Conclusions

The primary objective of this research project was to examine the effectiveness of transpiration for simulation of structural deformations in steady and unsteady aeroelastic applications. The majority of the investigations were performed using a recently modified version of a highly integrated, finite element-based code for the multidisciplinary analysis of flight vehicles. A supplement to this code was developed in this study which allows for the generation of deflected meshes using modal superposition. This research demonstrated that the transpiration boundary condition has strong potential for applications in unsteady aeroelastic analysis, such as in the prediction of flutter boundaries. The following conclusions were reached during this investigation:

1. The transpiration boundary condition is effective in simulating even relatively large displacements over a wide range of Mach numbers. Some the results support the rationale presented for when transpiration will lose accuracy. However, there is no

strict criteria for when the transpiration boundary condition will breakdown. These results show that for applications similar to the ones presented, such as flutter prediction, transpiration can be a very effective tool in simplifying the analysis.

2. Solutions involving the application of a domain mesh can be sensitive to the refinement of the mesh. The researcher performing studies using domain meshes should investigate the sensitivity of the mesh to his or her particular application, and depending on the desired accuracy, employ the mesh that is the most practical.

3. The codes developed in this study, FROMOD and SOLMOD, can accurately and simply be used to perform surface deflections. In cases where a surface is significantly deflected from its original position before it begins to oscillate, it may be effective to use a surface deflection scheme such as this to deform the body and then perform the flutter investigation from this initial condition.

4.2. Recommendations

The cases of this study used relatively simple geometries, as compared to full body configurations. According to the transpiration concept, there should be little or no accuracy lost in using transpiration in more complex cases. However, in instances such as

intersecting shocks and surfaces, it would be interesting to see how the transpiration boundary condition performs.

Also, considering the findings on mesh sensitivity, it is recommended that any future studies using the transpiration boundary condition to compare simulated deflections with actual deflections begin with a documentation of the sensitivity of the solution to the mesh.

Finally, since the majority of these results compared computer simulations with one another, it may be advisable to compare with experimental results when available to confirm the results from the simulations.

BIBLIOGRAPHY

Anderson, D. A., Tannehill, J. C., & Pletcher, R. H. (1984). Computational Fluid Mechanics and Heat Transfer. New York: Hemisphere Publishing Corporation.

Batina, J. T. (1989). Unsteady Euler Airfoil Solutions Using Unstructured Dynamic Meshes. AIAA Paper 89-0115, American Institute of Aeronautics and Astronautics.

Bharadvaj, B. K. (1990). Computation of Steady and Unsteady Control Surface Loads in Transonic Flow. AIAA Paper 90-0935, American Institute of Aeronautics and Astronautics.

Dixon, S. C. (No date given). Comparison of Panel Flutter Results from Approximate Aerodynamic Theory with Results from Exact Inviscid Theory and Experiment, NASA TN D-3649.

Gupta, K. K. (1995). An Integrated, Multidisciplinary Finite Element Structural, Fluids, Aeroelastic, and Aeroservoelastic Analysis Computer Program. Edwards, CA: National Aeronautics and Space Administration.

Henne, P. A. (1990). Applied Computational Aerodynamics. Washington, DC: American Institute of Aeronautics and Astronautics, Inc.

Lighthill, M. J. (1958). On Displacement Thickness. Journal of Fluid Mechanics, 4(4), 383-392.

Malone, J. B. & Sankar, L. N. (1985). Unsteady Full Potential Calculations for Complex Wing-Body Configurations. AIAA Paper 85-4062, American Institute of Aeronautics and Astronautics.

Malone, J. B., & Sotomayer, W. A. (1984). Unsteady Aerodynamic Modeling of a Fighter Wing in Transonic Flow. AIAA Paper 84-1566, American Institute of Aeronautics and Astronautics.

Raj, P., & Harris, B. (1993). Using Surface Transpiration with an Euler Method for Cost-Effective Aerodynamic Analysis. AIAA Paper 93-3506, American Institute of Aeronautics and Astronautics.

Ruo, S. Y., & Sankar, L. N. (1988). Euler Calculations for Wing-Alone Configuration. Journal of Aircraft, 25(5), 436-441.

Sankar, L. N., Malone, J. B., & Schuster, D. (1987). Euler Solutions for Transonic Flow Past a Fighter Wing. Journal of Aircraft, 24(1), 10-16.

Sankar, L. N., Malone, J. B., & Tassa, Y. (1981). An Implicit Conservative Algorithm for Steady and Unsteady Three-Dimensional Transonic Potential Flows. AIAA Paper 81-1016, American Institute of Aeronautics and Astronautics.

Sankar, L. N., Ruo, S. Y., & Malone, J. B. (1986). Application of Surface Transpiration in computational aerodynamics. AIAA Paper 86-0511, American Institute of Aeronautics and Astronautics.

Thomson, W. T. (1988). Theory of Vibration with Applications (3rd ed.). New Jersey: Prentice Hall.

APPENDIX--ADDITIONAL DATA

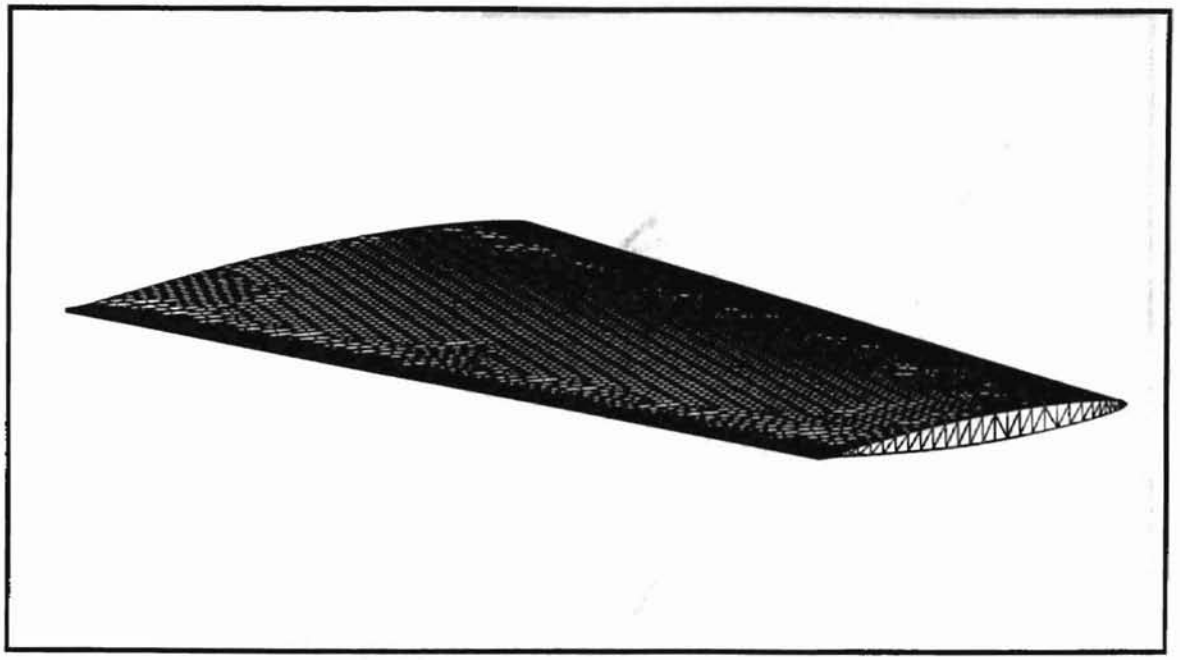

Figure A.1. AGARD Wing

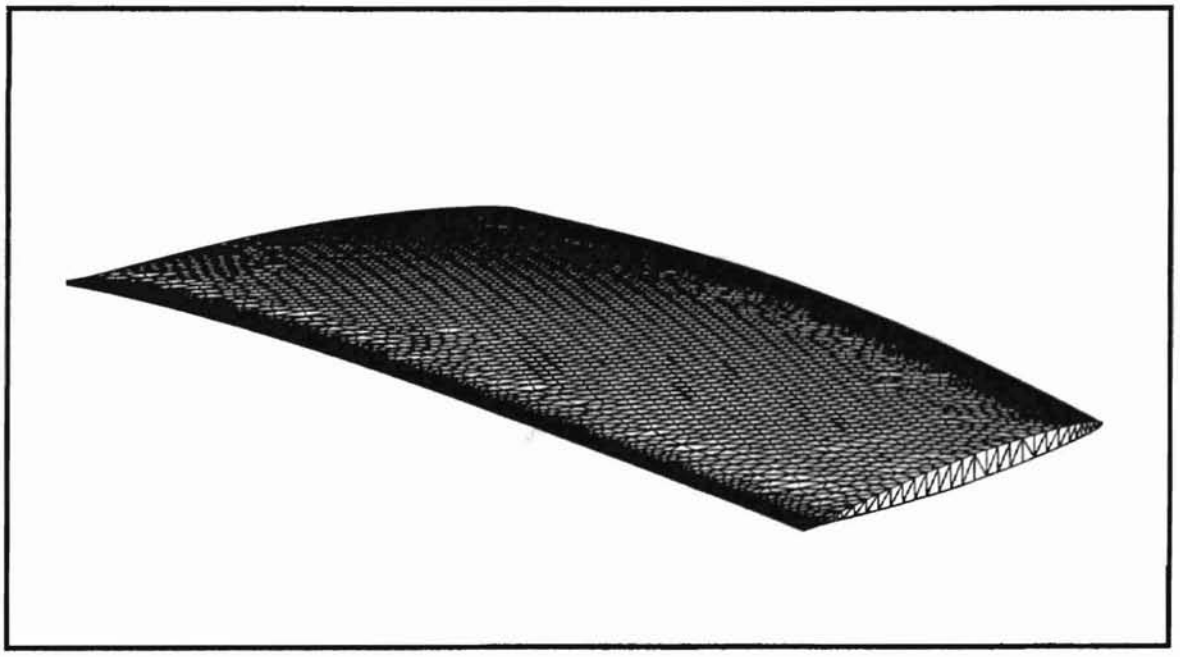

Figure A.2. Deflected AGARD Wing, 2.63 Units Bending and 0.33 Units Torsion

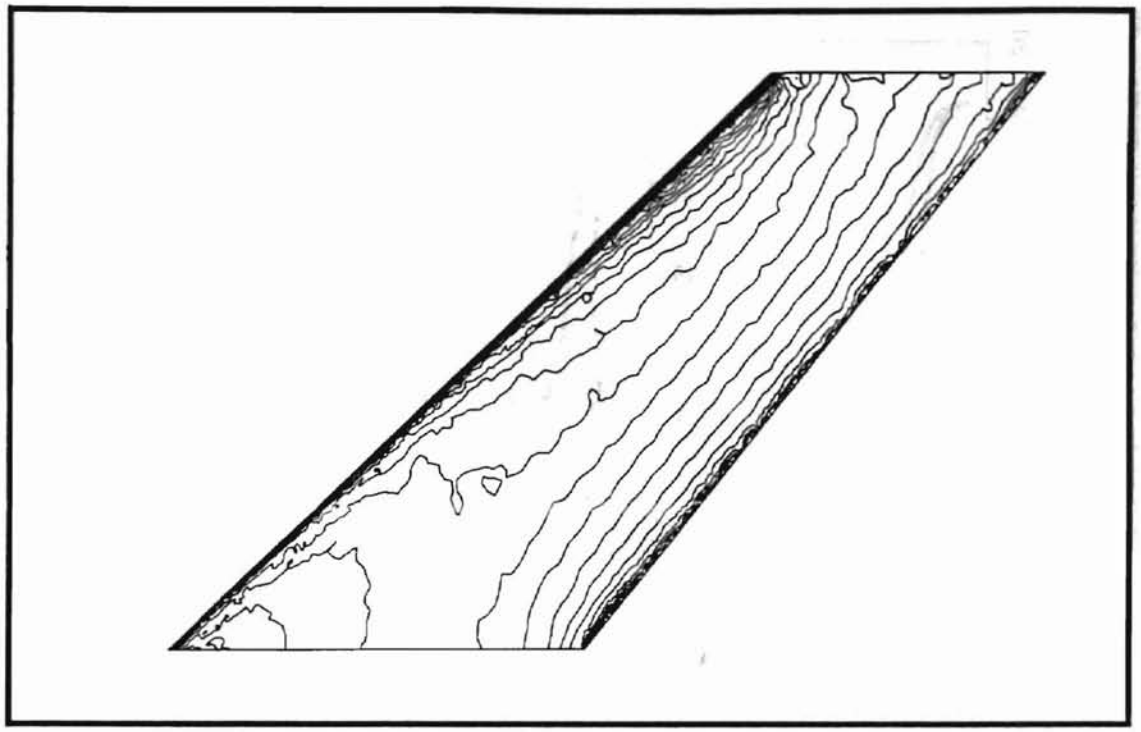

Figure A.3. Actual Pressure Contours, Mach 0.678

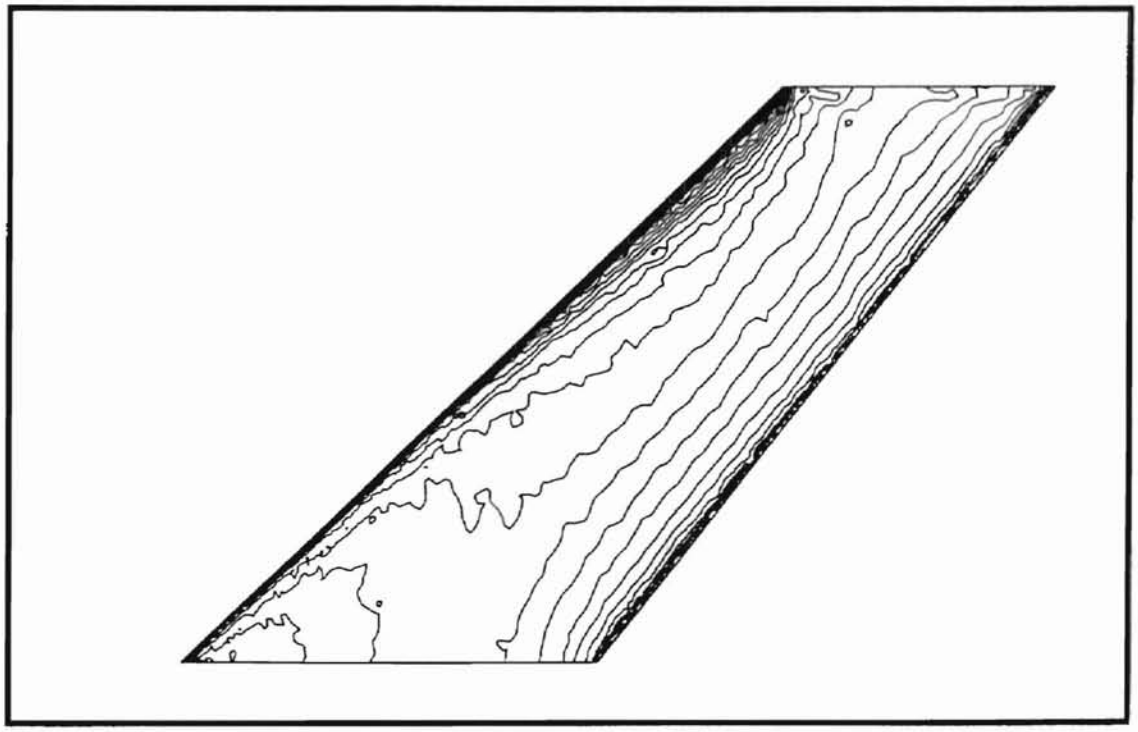

Figure A.4. Pressure Contours Using Transpiration, Mach 0.678

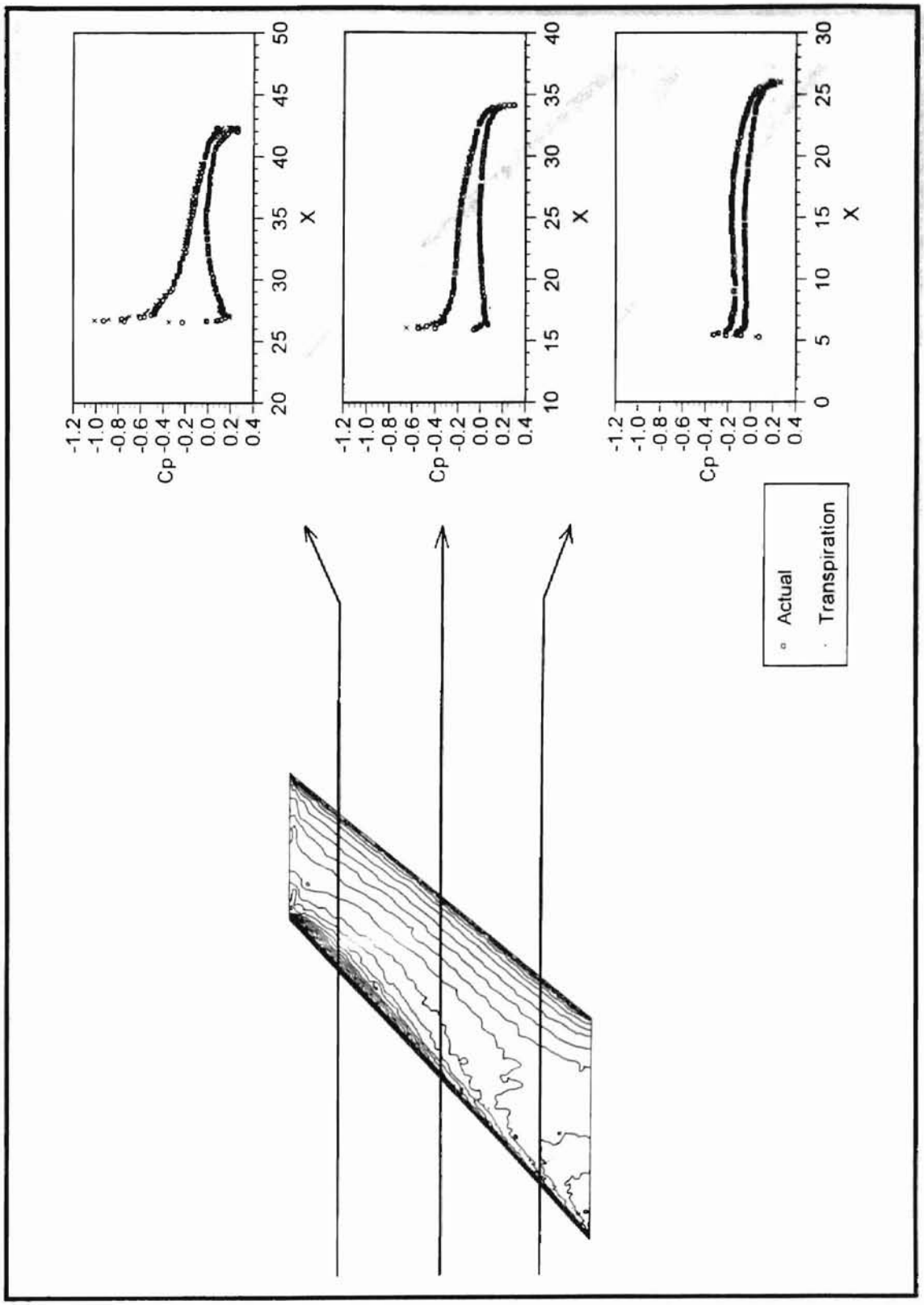

Figure A.5. Pressure Profiles, Mach 0.678

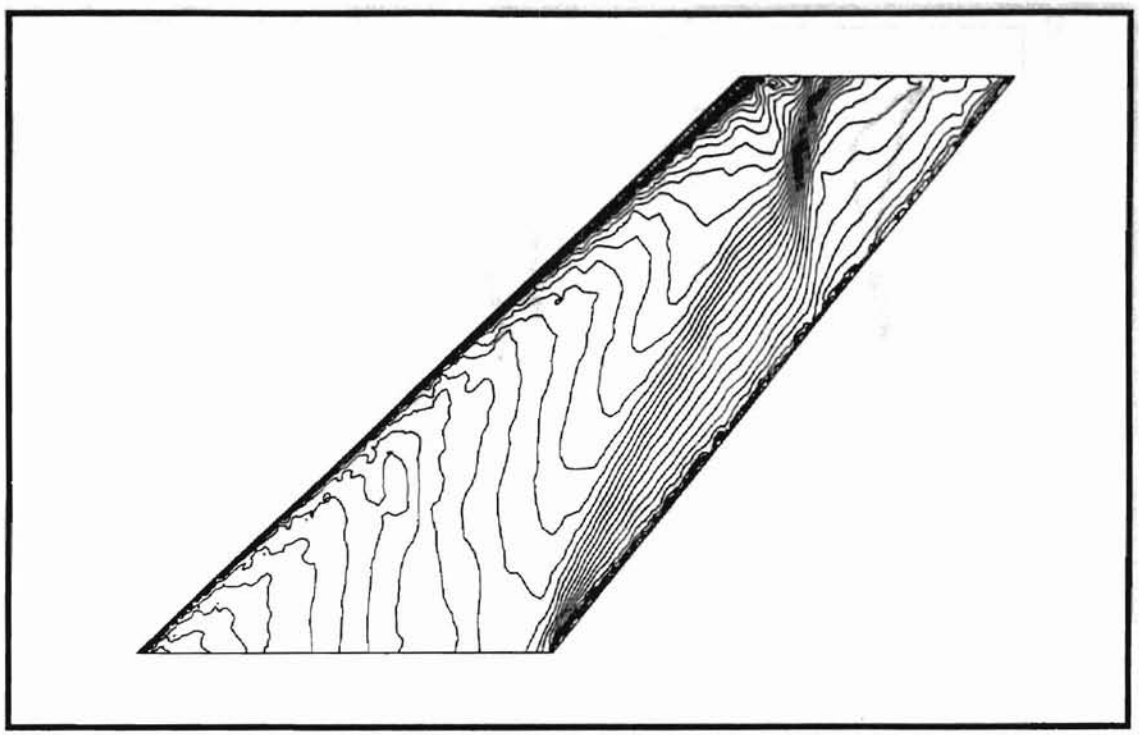

Figure A.6. Actual Pressure Contours, Mach 0.99

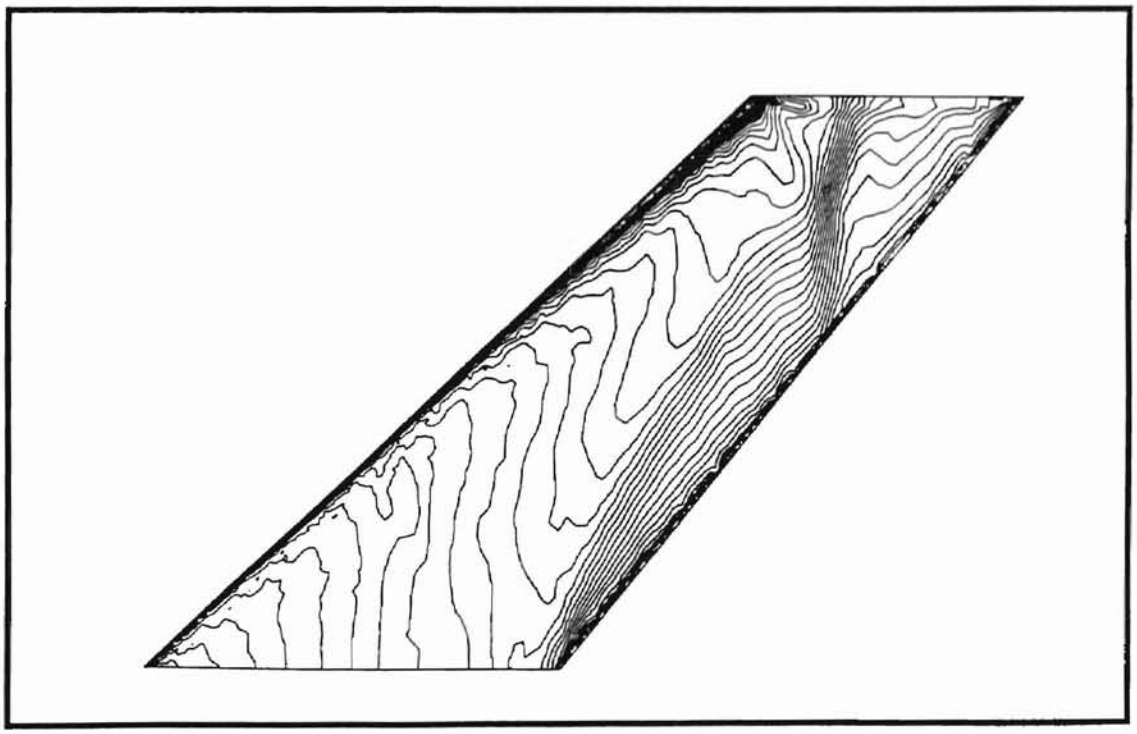

Figure A.7. Pressure Contours Using Transpiration, Mach 0.99

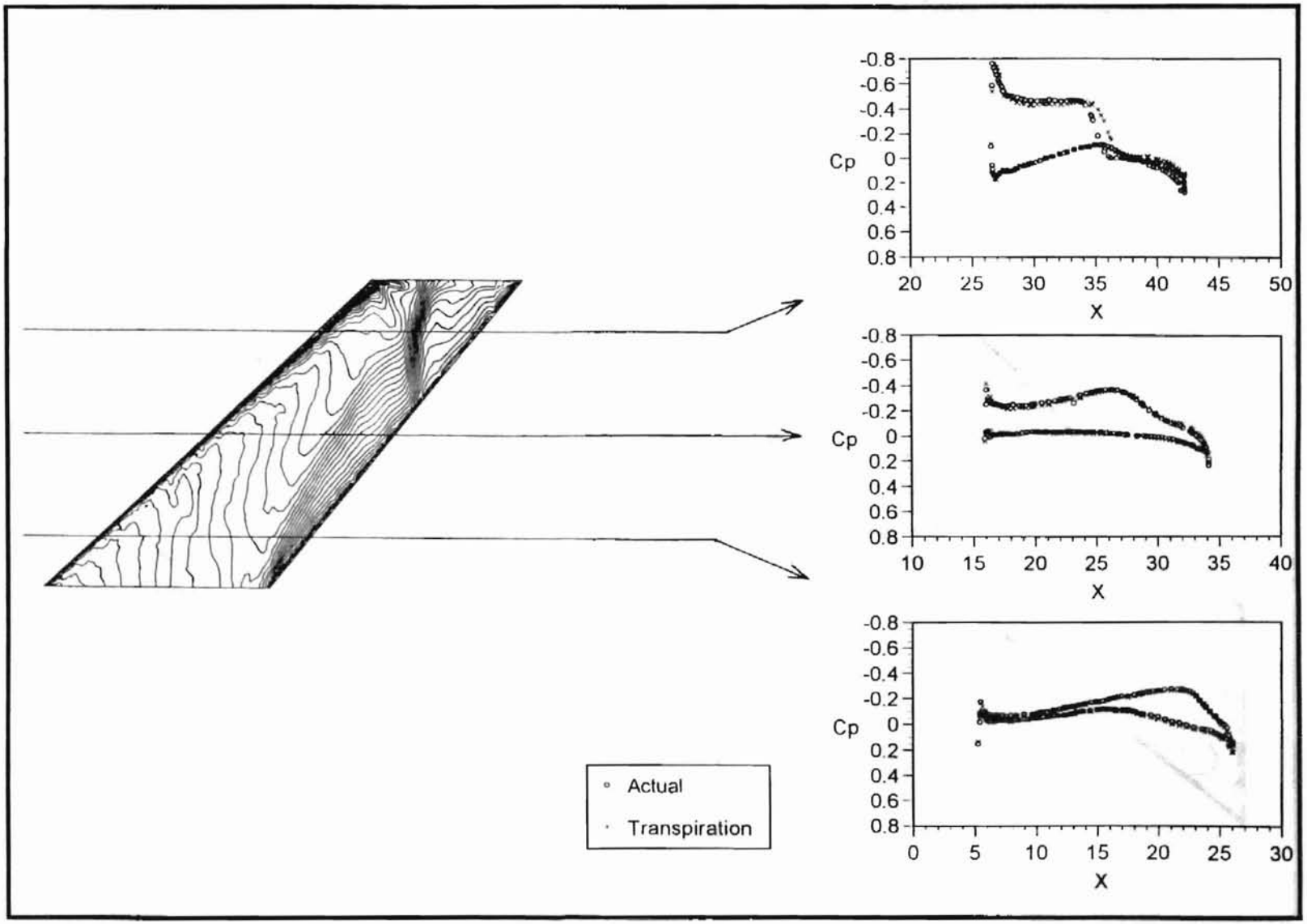

Figure A.8. Pressure Profiles, Mach 0.99

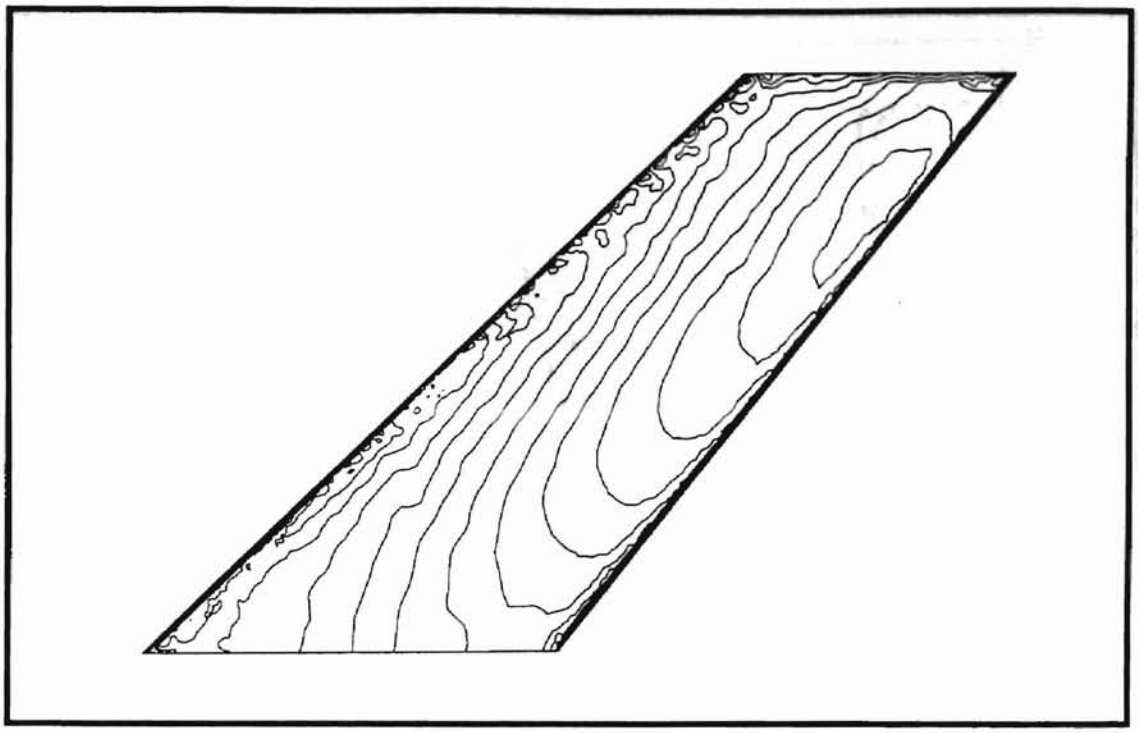

Figure A.9. Actual Pressure Contours, Mach 2.0

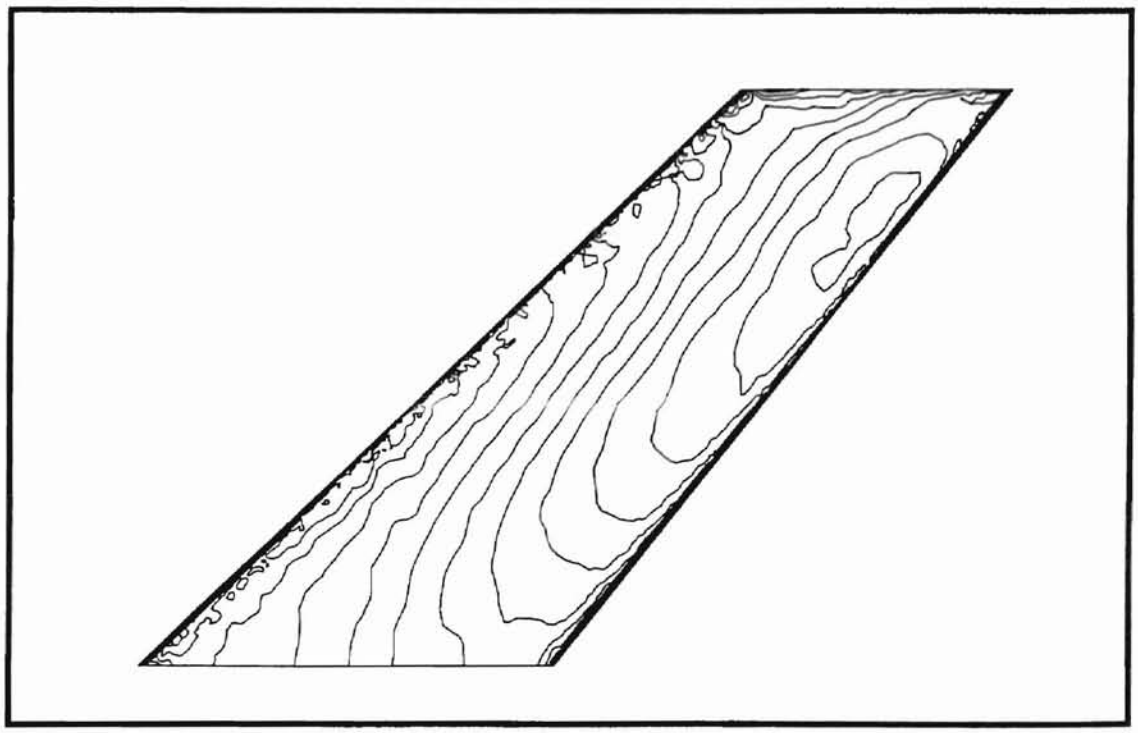

Figure A.10. Pressure Contours Using Transpiration, Mach 2.0

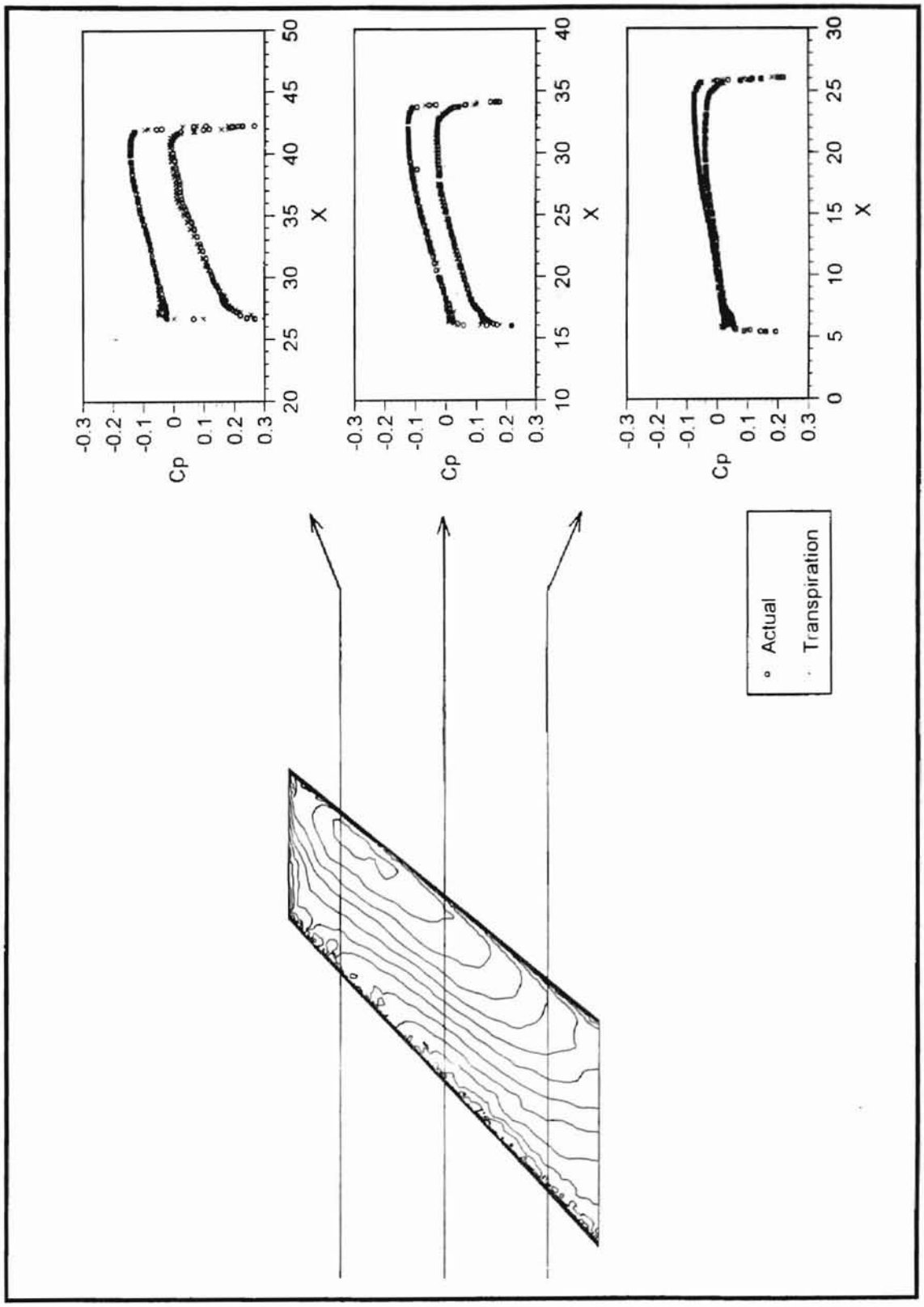

Figure A.11. Pressure Profiles, Mach 2.0

VITA 2

Clint C. Fisher

Candidate for the Degree of

Master of Science

Thesis: APPLICATION OF THE TRANSPIRATION METHOD FOR EFFICIENT AEROELASTIC ANALYSIS USING AN EULER SOLVER

Major Field: Mechanical Engineering

Biographical:

Personal Data: Born in Oklahoma City, Oklahoma, On September 18, 1970, the son of Lyndall C. and Barbara S. Fisher.

Education: Graduated from Putnam City West High School, Oklahoma City, Oklahoma, in May 1988; received Bachelor of Science degree in Mechanical Engineering with a minor in Mathematics from Oklahoma State University, Stillwater, Oklahoma in May 1993. Completed the requirements for the Master of Science degree with a major in Mechanical Engineering at Oklahoma State University in May 1996.

Experience: Employed by the Oklahoma Department of Transportation in an internship program; employed by Oklahoma State University as an undergraduate and as a graduate research assistant; Oklahoma State University, Department of Mechanical and Aerospace Engineering, 1992 to 1993 and 1994 to 1995.

Professional Memberships: American Institute of Aeronautics and Astronautics, American Society of Mechanical Engineers.